Application of a refined grid global model for operational wave forecasting

Forecasting Research
Technical Report No: 614

November 2016
Andy Saulter, Chris Bunney and Jian-Guo Li

Contents

Executive Summary

In November 2016 (at Operational Suite 38) the Met Office introduced a new global configuration of its wave forecast model. The model is based on WAVEWATCH III version 4.18. The configuration uses a Spherical Multiple-Cell (SMC) grid, with refined cell scales reducing from 25km in the open ocean to up to either 6km or 3km at the coastline. Source term physics follow the parameterisations described by Ardhuin et al. (2010). The refined grid method has been used in order to improve overall model accuracy (through providing a better description of coastline and island masks) whilst retaining model efficiency, and should have the additional benefit of enabling good quality forecasts to be generated in coastal waters without the requirement to set up and run nested regional models.

This report documents the provenance of the SMC grid model, describes the new global configuration and presents results from trials that were used to confirm the new configuration's quality and suitability as an operational wave forecast model upgrade. Comparisons between the new configuration and a 35km resolution global model, run operationally during the trials period, show a major overall improvement. For example, significant wave height errors were reduced from 18% of the background signal in the operational model to 14% in the new configuration, representing an improvement of over 20%. The model's utility for regional forecasting has also been demonstrated, with more modest improvements in performance found versus the Met Office European regional wave model (resolved at 8km). The changes in model quality result from a combination of both the grid and source term updates, with the most notable impact being a reduction in large over-prediction errors during storms.

1. Introduction

Within its role as the UK's National Meteorological Service, the Met Office provides forecasts from an operational global wave model. In addition to providing boundary conditions for higher resolution regional wave models, data from the global model are used in products generated by other meteorological services, commercial and defence forecasters for marine operations decision making.

Running a wave model covering a global domain can be computationally expensive. This usually leads to a trade-off where the model is capable of an accurate reproduction of wave conditions in open waters several 10s of kilometres from the coastline, but is of lower quality close to the coast and in shelf seas with limited fetches. Where a forecast is required for such inshore waters areas, a regional configuration may need to be created, leading to the modelling team having to run and manage multiple model instances. The traditional use of regular latitude-longitude grids in wave models leads to computational inefficiencies, since the model's propagation time steps have to be set according to the smallest model grid cell sizes in order for the model to remain stable (i.e. to satisfy the Courant-Friedrichs-Lewy, or CFL, criterion). In a global model these cells are found at high latitudes and can have a longitudinal size that is a factor of four (or more) times smaller than that of the equatorial cells (i.e. for a grid that extends beyond latitudes of 75°).

Both of these issues can be mitigated through use of a refined grid, in which model cell sizes (and time steps) can be varied in order to achieve both computational efficiencies and improved land-sea mask/bathymetry representation in coastal waters. Li (2011 and subsequent papers, see Section 2) proposed and implemented a Spherical Multiple-Cell (SMC) grid refinement method in WAVEWATCH III (at version 4.18; Tolman, 2014). This type of grid has been adopted in development of the Met Office's wave ensemble forecast system for the Atlantic-UK region (Bunney and Saulter, 2015) and the new global wave model described in this document.

The purpose of this report is to provide details of the new global configuration and present preliminary validation results, in the form of trials comparisons with present operational wave models, in-situ and remote sensed observations. Section 2 introduces the concepts underpinning the SMC grid wave model and identifies published research for readers interested in understanding the methods in further detail. Section 3 provides details of the global model configuration and notes the post processing methods applied to the raw model data in order to make it compatible with downstream Met Office research and forecasting systems. Section 4 describes the model trials process and summarises results. The results and perceived benefits of adopting the new global wave model configuration as the Met Office’s operational forecast model are discussed in Section 5.

2. Model provenance

Wave model configurations used for global or large regional area forecasts use a significant proportion of their computational time calculating the propagation of spectral wave energy through the model's spatial grid. Since WAVEWATCH III's first public release (Tolman, 1999), a number of grid schemes have been added to the model's options in order to optimise the time spent on propagation. For example, a multi-grid version of the model enables two way nesting of high resolution regional grids with a coarser model (Tolman, 2008); a rotated grid option is used to limit differentials between high and low latitude cells in a regional model (Tolman, 2014); an unstructured grid option optimises coastal bathymetry representation versus computation time for high resolution limited area applications (Roland et al., 2009).

Li (2011) first proposed the use of a Spherical Multiple-Cell (SMC) grid as a method to reduce limitations imposed by the CFL criterion at high latitudes within a global wave model. The method followed the reduced grid of Rasch (1994), where longitudinal cell sizes are doubled at each latitude (ϕ) when:

$$\cos\phi = 1/2^n \text{ , for n=1,2,3 etc..}$$

Li (2011) notes that the resulting relaxation of the CFL criterion introduces significant efficiencies versus a regular grid. A reduced grid SMC wave model, resolved at approximately 50km, has been employed at the Met Office to generate a global wave hindcast covering the period 1980 to present (Leonard-Williams and Saulter, 2013; Mitchell et al., 2016).

A further, and particularly useful, feature of the SMC grid is that it can also handle local refinement; for example to incorporate high resolution regions or coastal cells within the model grid. The method is similar to that used in adaptive mesh refinement, or the quadtree grid (Popinet et al., 2010), except that SMC grid refinement is static and can be extended to use single high resolution cells at coastlines. The cell refinement is achieved by using one-dimensional cell and face arrays which are sorted by size. These arrays describe location, cell size and adjacent cells for exchange of wave energy. Since the SMC grid uses rectangular cells, it remains compatible with the efficient explicit propagation schemes used in regular grid models. For example, papers published by Li (2011, 2012) have used a second order upstream non-oscillatory scheme (UNO2; Li, 2008), whilst the third order scheme of Tolman (2001) has been introduced as an option for the SMC grid in the forthcoming public release of WAVEWATCH III at version 5. In order to work efficiently with grid cells at different

resolutions, the SMC model extends WAVEWATCH III's use of variable time-stepping for propagation of different spectral frequencies to apply different time steps for different cell resolutions.

Li (2012) evaluated the numerical robustness of the multi-resolution SMC grid in WAVEWATCH III using a series of idealised propagation tests on a global 25-12-6km grid. Li and Saulter (2014) demonstrated a practical application through a comparison between the 25-12-6km model, a 35km resolved regular grid global wave model and a nested 4km regional model for the UK. Bunney and Saulter (2015) document the use of an Atlantic 25-12-6km SMC model in a short range wave ensemble prediction system.

The unstructured grid form also means that the model is able to resolve issues related to the singularity at the poles. Li (2016) demonstrated the concept by adding an arctic sub-grid within a global SMC wave model, running idealised propagation tests and making comparisons with observed wave height data at high northern hemisphere latitudes.

3 The S36125 Global Wave Model configuration for Operational Suite 38

The configuration details below relate to an implementation of the model using WAVEWATCH III version 4.18, after some minor bug fixes and Met Office specific alterations to partitioning and post-processing schemes (see Section 3.2).

3.1 Grid scheme

The Operational Suite 38 (OS38) configuration is based on a four-tier SMC grid refinement where the coarsest (open waters) cells are resolved at approximately 25km in mid-latitudes (0.35° longitude by 0.23° latitude) and reduce by a factor of two to 12km, 6km and 3km. From here on the configuration will be denoted as S36125. The use of the finest cell resolution (3km) has been restricted to European waters only in order to reduce computational costs. Presently the cell refinement is used to best represent the coastal mask, and does not introduce additional resolution over shoals or areas with highly variable bathymetry (i.e. where refraction effects might significantly alter the wave field). Over the European region (covering approximately 15°W to 45°E and 30°N to 63°N) the coarsest cell size has been set to 12km, so that the model can exploit the full detail of the next Met Office global atmosphere model in this part of the domain (an anticipated increase in horizontal resolution to approximately 12km in 2017). At higher latitudes, longitudinal cell sizes are doubled (by a factor of 2 at 60°N, 4 at 75°N, 8 at

83°N) in order to support a larger CFL time-step than would be permitted by a regular latitude-longitude grid.

Figures 1-4 illustrate how the cell refinement works. Figure 1 shows the grid over the Hawaiian Islands. In this and subsequent figures, the box lines define the extent of each grid cell. The largest cells (25km) cover much of the open ocean around the islands, but around the coastline cell sizes are initially halved to the 12km scale and then halved again, directly adjacent to the coast, using the 6km cell size. In addition to improving the coastal mask around the islands, the cell scaling also enables resolution of inter-island channels, e.g. between Maui, Moloka'i and Lanai. Figure 2 shows the detail provided by the grid on a much larger scale, covering the Caribbean and isles bordering the Atlantic Ocean. The distribution of cell sizes indicates that large areas of the seas in this region will be dealt with by the most computationally efficient (largest) cells, whilst the smaller cells aim to accurately represent the barrier effects of islands bordering the Atlantic.

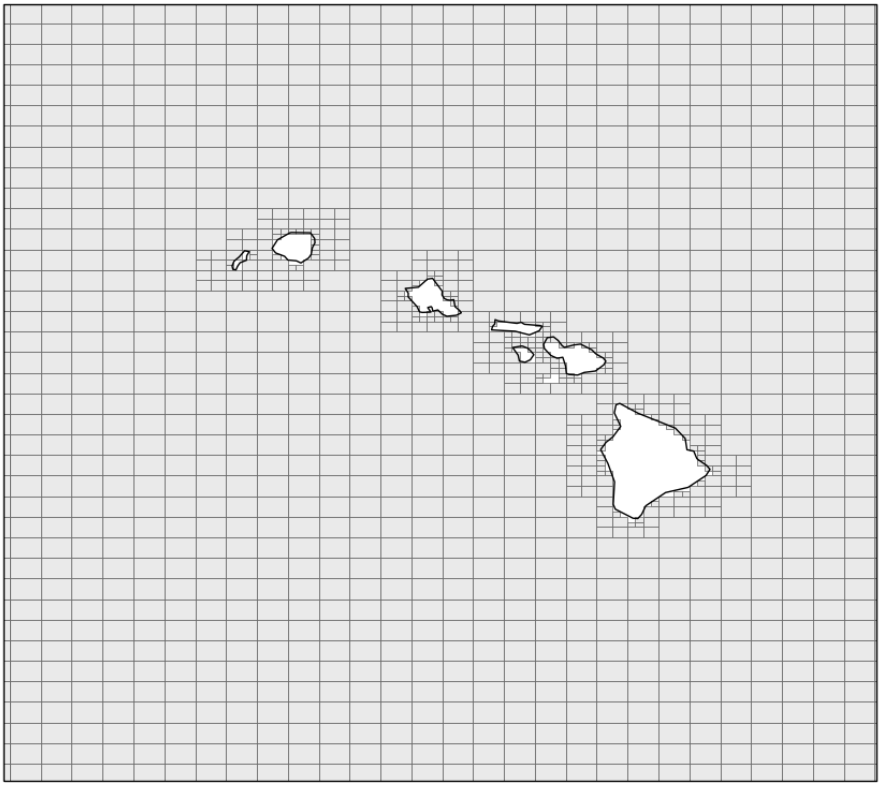

Figure 1. Layout of 25-12-6km grid cells in the S36125 grid around the Hawaiian Islands.

Figures 3 and 4 are show how the grid is set up in the 12-6-3km European region of the model. Figure 3 is a wide area view of the UK. In addition to capturing details of the coastline and islands, this figure also illustrates the behaviour of the grid at latitude 60°N,

where longitudinal cell size is doubled in order to support a larger CFL timestep. The zoom over northeast Scotland and the Orkney and Shetland Isles is indicative of the high levels of coastal definition achieved by the model in the European zone. These are particularly important for achieving correct representation of fetch restrictions in coastal waters; such as in the Moray Firth and Firth of Forth during prevailing westerly wind conditions. The Pentland Firth is also resolved by multiple cells in the model, although the addition of current information would be needed in order to properly represent wave growth and dissipation in this highly dynamic channel.

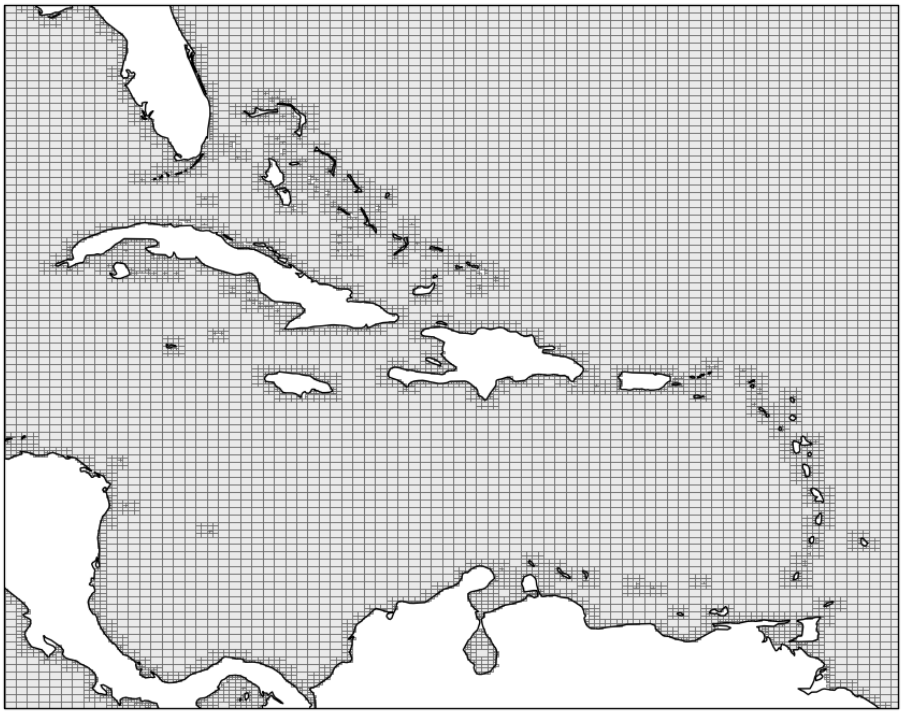

Figure 2. Layout of 25-12-6km grid cells in the S36125 grid for the Caribbean.

At present, forcing data for these grids are pre-processed and applied at the scale of the coarsest wave model cells only. For example, the wind data used to generate waves in a highly fetch constrained area, such as the Firth of Forth, will be a uniform application of a 25km wind field that is interpolated from the Met Office global atmosphere model. As part of ongoing development, work will be undertaken to enable the SMC models to make use of higher resolution forcing fields at the coast by applying cell-size specific interpolation and mapping of forcing data direct onto the multiple-resolution grid's sea-points. This should further improve the model's coastal performance.

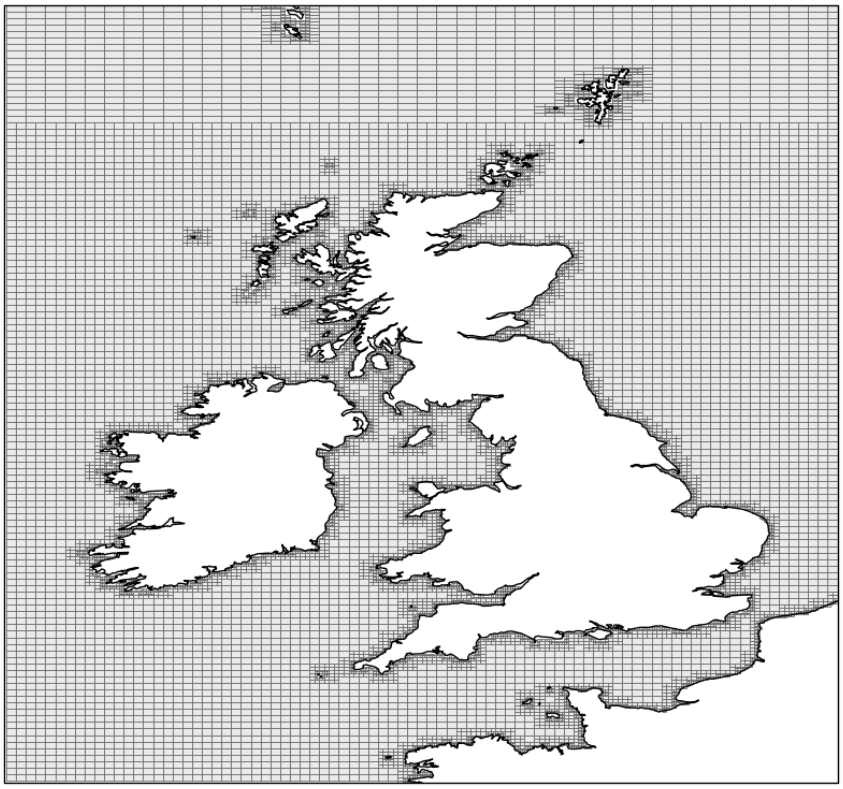

Figure 3. Layout of 12-6-3km grid cells in the S36125 grid for the UK.

Figure 4. Zoom showing layout of 12-6-3km grid for northeast Scotland, Orkney and Shetland.

3.2 Source terms and propagation scheme

The S36125 spectral grid is defined using 30 frequency bins (geometrically spaced using a multiplier of 1.1 and starting at 0.04118Hz, covering wave periods from 25 to 1.5 seconds) and 36 direction bins. After various trials, the best source term combination for this configuration was found to be based on the WAVEWATCH III version 4.18 ST4 package, which uses wave growth and dissipation parameterisations following Ardhuin et al. (2010). The tuning parameter BETAMAX, which provides an overall control on the input wind stress, has been revised to 1.36 for compatibility with Met Office wind data; otherwise the ST4 default values are used. Nonlinear wave-wave 'quadruplet interactions', which shift wave energy toward lower frequencies, are parameterised using the Discrete Interaction Approximation of Hasselmann et al. (1985). The propagation method incorporated with the SMC grid uses a second order upstream non-oscillatory scheme (Li, 2008), with Garden Sprinkler Effect alleviation using a hybrid of the 'swell-age' diffusion scheme of Booij and Holthuijsen (1987) and a 1-2-1 weighted averaging scheme similar to that of Tolman (2002).

3.3 Post processing

In order to render the model grid at its native resolution, the ww3_ounf.ftn module of the WAVEWATCH III code has been adapted to create 'sea point only' netCDF files. These files comprise two-dimensional data arrays (time, cell index) for model output parameters, with accompanying metadata describing cell latitude and longitude plus cell size. Met Office operational forecasting systems are not presently configured to receive data in this form, so a second post-processing step is run in the operational suite to create a regular latitude-longitude product based on the model's coarsest resolution (25km). This is based on interpolation code which maps from the SMC native grid to any regular grid specified at one of the model's resolution tiers.

In line with other operational Met Office models, and following a requirement stipulated by Met Office marine forecasters, the partitioning scheme in the model has been adapted such that wind-sea is calculated based only on that part of the spectrum where wave energy travels slower than the (co-directed) wind speed. The remnant energy is partitioned using a water-shedding method in order to identify multiple swell components. For operational purposes, the wind-sea, primary, secondary and tertiary swells are returned in the model output files.

4 Validation trials

4.1 Trials procedure

Ocean surface waves are an example of a 'forced-dissipative system' in which the wave growth and dissipation is a response to the atmospheric forcing that is applied to the ocean, whilst the waves also propagate energy away from the forcing zone. In practise the system's primary sensitivity is to the wind forcing such that, in modelling terms, the potential for any wave forecast to drift is governed by the behaviour of the forcing atmospheric model. On this basis, the quality of the wave model can be assessed by applying a 'best available' wind forcing dataset (in this case assumed to be the Met Office global atmosphere model analysis fields) and comparing resulting wave parameters with observations.

Two observation sources have been used. The de-facto standard for wave measurement is in-situ data, using various instruments mounted on floating buoys and fixed marine platforms (e.g. oil installations). A global dataset of these measurements is collated and quality controlled each month under the WMO-IOC Joint Commission On Marine Meteorology's operational Wave Forecast Verification Scheme (Bidlot et al. 2007, hereafter referred to as the JCOMM-WFVS). Over 400 measurement sites are registered in the system, although these are predominantly based in the northern hemisphere and within several hundred kilometres of the coasts of North America and Europe. The second source of observed data was taken from satellite altimeter missions. These have been conveniently aggregated, quality controlled and calibrated by CERSAT (Queffeulou, 2013) and are available for public download from ftp://ftp.ifremer.fr/ifremer/cersat/products/swath/altimeters/waves/data .

A one-year validation period covering September 2014 to August 2015 was used to validate the model. This period was chosen as a full calendar year during which observations were available from both data sources and post a substantial upgrade made to the Met Office atmospheric forecast model in July 2014 (at OS34). In addition to the observations, the validation procedure also compared the S36125 configuration with versions of the global wave model that were running operationally during this period. The operational global wave model was based on version 3.14 of WAVEWATCH III (Tolman, 2009), used a 35km resolved 'strip grid' and was subject to an update to its source term physics in February 2015 (OS35), when the model was switched from using the ST2 source terms of Tolman and Chalikov (1996) to a WAM Cycle-4 (Komen et al., 1994; ST3) based scheme. The model and physics set ups are

further documented in Saulter (2015) and the model will be denoted as the OS34-35 model from here on.

Within the trials work a number of metrics were used to review the model performance. The key metrics discussed in this report are:

- Model – observation bias; $Bias = \mathrm{E}\left|x_{model} - x_{observation}\right|$
- Model – observation root mean squared error (RMSE); $RMSE = \sqrt{\mathrm{E}\left|\left(x_{model} - x_{observation}\right)^2\right|}$
- Normalised model standard deviation (assesses signal in model versus that in the observations); $NormStd = \sqrt{\frac{\mathrm{E}\left|x_{model}^2\right|}{\mathrm{E}\left|x_{observation}^2\right|}}$
- Pearson correlation; $\rho = \frac{\mathrm{E}\left|x_{model}\,x_{observation}\right| - \mathrm{E}\left|x_{model}\right|\mathrm{E}\left|x_{observation}\right|}{\sqrt{\mathrm{E}\left|x_{model}^2\right| - \mathrm{E}\left|x_{model}\right|^2}\sqrt{\mathrm{E}\left|x_{observation}^2\right| - \mathrm{E}\left|x_{observation}\right|^2}}$

In the tables provided in this report both bias and RMSE scores have been normalised in order to enable some cross comparison of results in specific regions. RMSE is normalised relative to the root mean square value of the observations, so that the error signal is expressed in terms of the observed signal for each parameter validated. A number of authors argue for different approaches to be used in order to improve the robustness of this statistic (e.g. Mentaschi et al., 2013) but, for the present, the literature is inconsistent in this regard, whilst the approach here enables some direct comparisons with previous studies; e.g. spatial results presented by Ardhuin et al. (2010) and Saulter (2015). Bias is normalised relative to the observed mean, so that the systematic error of the model is expressed in terms of the background observed sample climate.

4.2 In-situ data comparisons versus OS34-35 global wave model

The JCOMM-WFVS dataset enables a comparison of significant wave height (Hs), peak period (Tp) and mean zero-upcrossing period (Tz). In addition, wind speed (Ws) data are available, enabling some assessment of the quality of the forcing data for these trials. Results of the comparisons between observations and both S36125 and OS34-35 models for the full dataset and specific regions are given in Tables 2-5. The in-situ sites identified in each regional analysis are shown in the figures in Appendix A.

Table 2. Wind speed (Ws) statistics for global and regional JCOMM-WFVS data. Observed mean and standard deviation values are in ms^{-1}, other statistics are normalised according to the description in section 4.1.

	Observed		S36125-ST4				G35-OS			
Region	**Mean**	**StDev**	**RMSE**	**Bias**	**StDev**	**Corr**	**RMSE**	**Bias**	**StDev**	**Corr**
All	6.89	3.49	**0.16**	**0.02**	**1.07**	**0.94**	0.17	0.03	1.07	0.94
Irish Sea	7.23	3.19	0.18	0.09	1.20	**0.95**	0.17	0.08	1.18	0.95
North Sea	8.31	3.92	**0.13**	**0.00**	1.06	**0.96**	0.13	0.00	1.06	0.95
UK Western Approaches	8.15	3.55	**0.15**	**0.08**	1.14	**0.96**	0.15	0.08	1.14	0.96
Iberian Atlantic	5.99	3.12	**0.22**	0.12	1.16	**0.94**	0.23	0.11	1.16	0.92
West Mediterranean	5.56	3.71	**0.24**	**0.06**	**1.10**	**0.92**	0.26	0.08	1.11	0.91
East Mediterranean	5.44	2.88	**0.32**	-0.09	**1.04**	0.80	0.32	0.05	1.14	0.80
Brazil	6.96	2.86	**0.28**	0.03	1.07	**0.75**	0.28	0.03	1.06	0.74
Caribbean	7.34	2.35	0.08	**0.02**	1.01	0.97	0.08	0.02	1.01	0.97
Northwest Atlantic	7.17	3.66	**0.15**	**0.07**	1.10	**0.96**	0.16	0.08	1.10	0.96
Central West Atlantic	6.25	2.38	0.11	**0.02**	1.06	0.96	0.11	0.03	1.06	0.96
US East Coast	6.65	3.13	0.15	**0.03**	**1.07**	0.95	0.14	0.03	1.08	0.95
Korea-Japan	5.91	3.53	**0.24**	**-0.06**	**0.99**	**0.90**	0.26	-0.07	0.99	0.87
India	4.92	2.23	0.23	**0.09**	1.12	0.89	0.23	0.09	1.12	0.89
Hawaii	6.69	2.29	**0.11**	0.05	**1.04**	**0.96**	0.11	0.05	1.04	0.96
US West Coast	6.19	3.13	**0.17**	**0.01**	**1.07**	**0.93**	0.18	0.01	1.08	0.93
Northeast Pacific	7.24	3.47	0.14	**0.05**	1.11	0.97	0.14	0.05	1.10	0.97
Gulf of Mexico	5.82	2.55	**0.14**	**0.02**	**1.08**	**0.95**	0.14	0.02	1.08	0.94

Table 3. Significant wave height (Hs) statistics for global and regional JCOMM-WFVS data. Observed mean and standard deviation values are in m, other statistics are normalised according to the description in section 4.1.

	Observed		S36125-ST4				G35-OS			
Region	**Mean**	**StDev**	**RMSE**	**Bias**	**StDev**	**Corr**	**RMSE**	**Bias**	**StDev**	**Corr**
All	1.82	1.23	**0.14**	**-0.02**	**0.98**	**0.97**	0.18	0.03	1.04	0.95
Irish Sea	1.15	0.77	**0.16**	**-0.04**	**1.03**	**0.96**	0.19	-0.06	0.95	0.94
North Sea	2.04	1.33	**0.09**	**0.02**	**0.98**	**0.99**	0.13	0.06	1.04	0.98
UK Western Approaches	3.08	1.79	**0.09**	**0.00**	**1.00**	**0.98**	0.14	0.03	1.08	0.97
Northeast Atlantic	2.82	1.75	**0.13**	**-0.02**	**0.97**	**0.97**	0.18	0.04	1.05	0.95
Iberian Atlantic	2.14	1.27	**0.14**	**0.00**	**0.96**	**0.96**	0.18	0.04	1.04	0.94
West Mediterranean	1.09	0.90	**0.17**	-0.09	**1.00**	**0.97**	0.20	-0.01	1.09	0.96
East Mediterranean	1.02	0.78	**0.20**	-0.14	**0.96**	**0.96**	0.28	0.09	1.17	0.93
Australia West Coast	2.04	0.64	**0.12**	**0.02**	**0.88**	**0.91**	0.20	0.10	1.18	0.86
Australia East Coast	1.82	0.93	0.27	-0.13	0.71	0.85	0.22	-0.06	0.85	0.89
Brazil	2.01	0.74	**0.18**	-0.04	0.85	**0.86**	0.19	-0.01	0.96	0.85
Caribbean	1.47	0.63	**0.14**	**0.05**	**0.97**	**0.94**	0.18	0.10	1.03	0.93
Northwest Atlantic	1.98	1.30	**0.14**	-0.01	0.89	**0.97**	0.15	-0.01	0.94	0.96
Central West Atlantic	1.80	0.62	**0.09**	**0.01**	0.91	**0.96**	0.11	-0.02	1.00	0.94
US East Coast	1.40	0.80	**0.14**	0.01	0.95	**0.96**	0.16	-0.01	0.98	0.95
Korea-Japan	1.12	0.83	**0.25**	-0.17	0.89	**0.93**	0.26	-0.03	0.96	0.91
India	1.62	0.88	**0.14**	-0.03	0.89	**0.96**	0.16	-0.01	0.91	0.95
Hawaii	2.10	0.65	**0.12**	**0.03**	**0.96**	**0.92**	0.18	0.10	1.06	0.87
US West Coast	2.03	0.91	**0.12**	**-0.03**	0.93	**0.96**	0.16	0.03	0.99	0.93
Northeast Pacific	2.43	1.22	**0.11**	**-0.01**	0.94	**0.97**	0.14	0.01	0.99	0.95
Gulf of Mexico	1.02	0.61	**0.17**	-0.02	0.97	**0.94**	0.18	0.01	1.00	0.94

Table 4. Peak wave period (Tp) statistics for global and regional JCOMM-WFVS data. Observed mean and standard deviation values are in seconds, other statistics are normalised according to the description in section 4.1.

	Observed		S36125-ST4				G35-OS			
Region	**Mean**	**StDev**	**RMSE**	**Bias**	**StDev**	**Corr**	**RMSE**	**Bias**	**StDev**	**Corr**
All	8.88	3.17	**0.24**	0.06	**1.12**	**0.78**	0.29	0.05	1.22	0.73
Irish Sea	4.70	1.38	**0.41**	**0.01**	**1.62**	**0.46**	0.48	0.06	1.71	0.31
North Sea	5.68	2.11	0.31	**0.06**	1.15	0.69	0.27	-0.06	0.99	0.72
UK Western Approaches	11.30	2.62	**0.09**	**-0.02**	0.95	**0.92**	0.12	-0.03	1.00	0.87
Northeast Atlantic	11.30	2.45	**0.08**	**-0.01**	**1.02**	**0.93**	0.12	-0.03	1.02	0.86
Iberian Atlantic	8.48	2.32	0.39	0.31	**1.14**	0.63	0.39	0.30	1.23	0.64
West Mediterranean	5.39	1.37	**0.22**	**0.02**	**1.27**	**0.73**	0.24	0.03	1.28	0.66
East Mediterranean	5.46	1.43	**0.23**	**-0.14**	**0.90**	0.71	0.26	-0.19	0.82	0.73
Australia West Coast	12.39	2.20	**0.16**	0.06	0.75	**0.58**	0.18	0.04	0.92	0.49
Australia East Coast	10.00	2.27	**0.19**	**-0.03**	**1.19**	**0.72**	0.22	-0.03	1.29	0.65
Brazil	8.87	1.88	**0.17**	-0.05	**0.94**	**0.67**	0.20	-0.04	1.13	0.62
Caribbean	7.12	1.40	**0.18**	**0.05**	**1.13**	**0.65**	0.20	0.05	1.19	0.61
Northwest Atlantic	8.29	2.07	**0.18**	**-0.01**	0.93	**0.72**	0.19	-0.03	1.02	0.71
Central West Atlantic	8.94	1.90	**0.13**	**0.01**	0.83	**0.79**	0.16	-0.01	1.08	0.73
US East Coast	7.71	2.10	**0.21**	**0.02**	0.93	**0.67**	0.23	-0.03	1.04	0.65
Korea-Japan	5.96	2.05	**0.30**	**0.10**	**1.26**	**0.71**	0.39	0.16	1.39	0.61
Hawaii	10.60	2.59	**0.26**	**0.11**	**1.13**	**0.58**	0.32	0.15	1.26	0.46
US West Coast	11.59	2.88	**0.24**	**0.10**	**1.06**	**0.60**	0.29	0.12	1.15	0.49
Northeast Pacific	10.26	2.63	**0.28**	**0.10**	**1.18**	**0.53**	0.34	0.12	1.33	0.43
Gulf of Mexico	5.84	1.31	**0.17**	-0.06	**0.92**	**0.70**	0.24	-0.04	1.14	0.52

Table 5. Mean zero-upcrossing wave period (Tz) statistics for global and regional JCOMM-WFVS data. Observed mean and standard deviation values are in seconds, other statistics are normalised according to the description in section 4.1.

	Observed		S36125-ST4				G35-OS			
Region	**Mean**	**StDev**	**RMSE**	**Bias**	**StDev**	**Corr**	**RMSE**	**Bias**	**StDev**	**Corr**
All	6.00	1.66	**0.14**	-0.08	**1.01**	**0.89**	0.15	-0.06	1.05	0.87
Irish Sea	5.09	1.51	**0.30**	**-0.21**	**0.75**	**0.63**	0.32	-0.23	0.69	0.58
North Sea	5.84	1.43	**0.16**	-0.09	0.88	**0.84**	0.16	-0.06	0.97	0.81
UK Western Approaches	7.07	1.59	**0.10**	-0.06	**0.99**	**0.95**	0.11	-0.05	1.08	0.92
Northeast Atlantic	6.55	1.58	**0.13**	-0.09	**0.99**	**0.92**	0.13	-0.06	1.06	0.89
Iberian Atlantic	6.92	1.77	**0.10**	-0.04	**1.07**	**0.95**	0.11	-0.04	1.12	0.92
West Mediterranean	4.27	1.00	0.17	-0.12	**1.05**	**0.88**	0.16	-0.09	1.16	0.86
East Mediterranean	4.34	0.88	**0.17**	-0.14	**1.12**	**0.89**	0.17	-0.03	1.34	0.76
India	5.98	1.27	**0.15**	**0.00**	1.21	**0.81**	0.15	-0.05	1.14	0.80

The results indicate a significant improvement in the agreement between the new model and the observations, particularly in terms of significant wave height. Figures 5-8 show scatter and quantile-quantile (QQ) relationships derived for, Ws, Hs, Tp and Tz across all JCOMM-WFVS sites where each parameter was measured and forecast by both models. Each figure follows the same format. The upper and middle panels show, respectively, the comparison between OS34-35 and S36125 model data against observed values. The bottom panel compares the model-observation errors from each system. Within each panel, the hexbin scatter diagram illustrates the distribution of time-matched data, with colour denoting population size, whilst the black symbols show the

(sample climate) QQ comparison. For the QQ data, each change in symbol denotes an order of magnitude increase in the percentile resolution (e.g. the change from circles to squares defines a shift from every 1% in the data sample to every 0.1%). The red dashed line illustrates a linear best fit for the scatter data, where the model prediction is defined as the independent variable. Statistics describing the observed, modelled and model-observation error distributions are provided in the panel on the right of each plot.

Since forcing data for OS34-35 and S36125 models are based on a bilinear interpolation of the same Met Office 10m wind fields onto their respective grids, wind speed verification should not be significantly different between the two systems. The global comparison (Figure 5) confirms that there are no major differences, although a very small improvement in wind speed bias and RMSE (order centimetres per second) is achieved for the new grid. Presumably this is either a result of better coastal masking in the S36125 configuration or a better match between wave and atmosphere model grids in the higher resolution European region. A feature of the QQ data for both models is an over-prediction of the observed wind speeds above the 90th percentile. The errors QQ plot (bottom panel of Figure 5) suggests that the key difference is a slight reduction in the number of under-prediction errors in the S36125 model, although this only really impacts the lower 0.01% tail of the error distribution.

The change in significant wave height performance is, as hoped, more marked. The overall statistics show a global improvement in Hs RMSE from 18% of the background signal for OS34-35 to 14% for S36125. This 4% change against background represents a relative improvement in the errors of over 20%. Figure 6 shows that a much tighter scatter comparison against observations is achieved by the S36125 model. The QQ data do not show any tendency for model over-prediction in the upper tail of the Hs distribution (which is a notable feature of the OS34-35 models above the 0.1 percentile). The errors comparison shows that the S36125 model is significantly less likely to generate a high over-forecast error, above the 1% tail of the error distribution. These large errors are most readily associated with prediction of large Hs values during major storms.

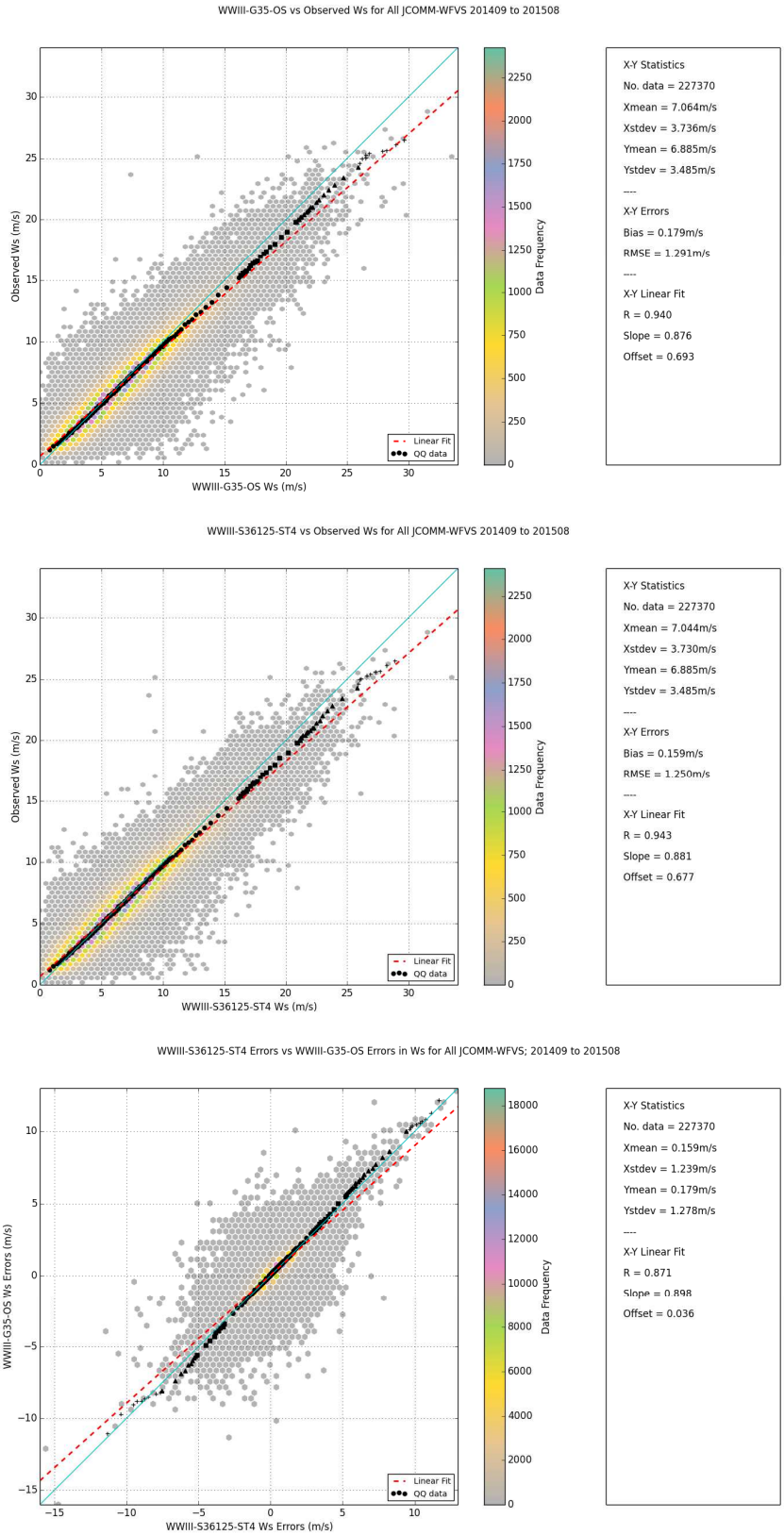

Figure 5: Wind speed QQ and scatter data for all JCOMM-WFVS in-situ sites. Top, comparison against OS34-35 model; centre, comparison against S36125 model; bottom, comparison of OS34-35 versus S36125 errors.

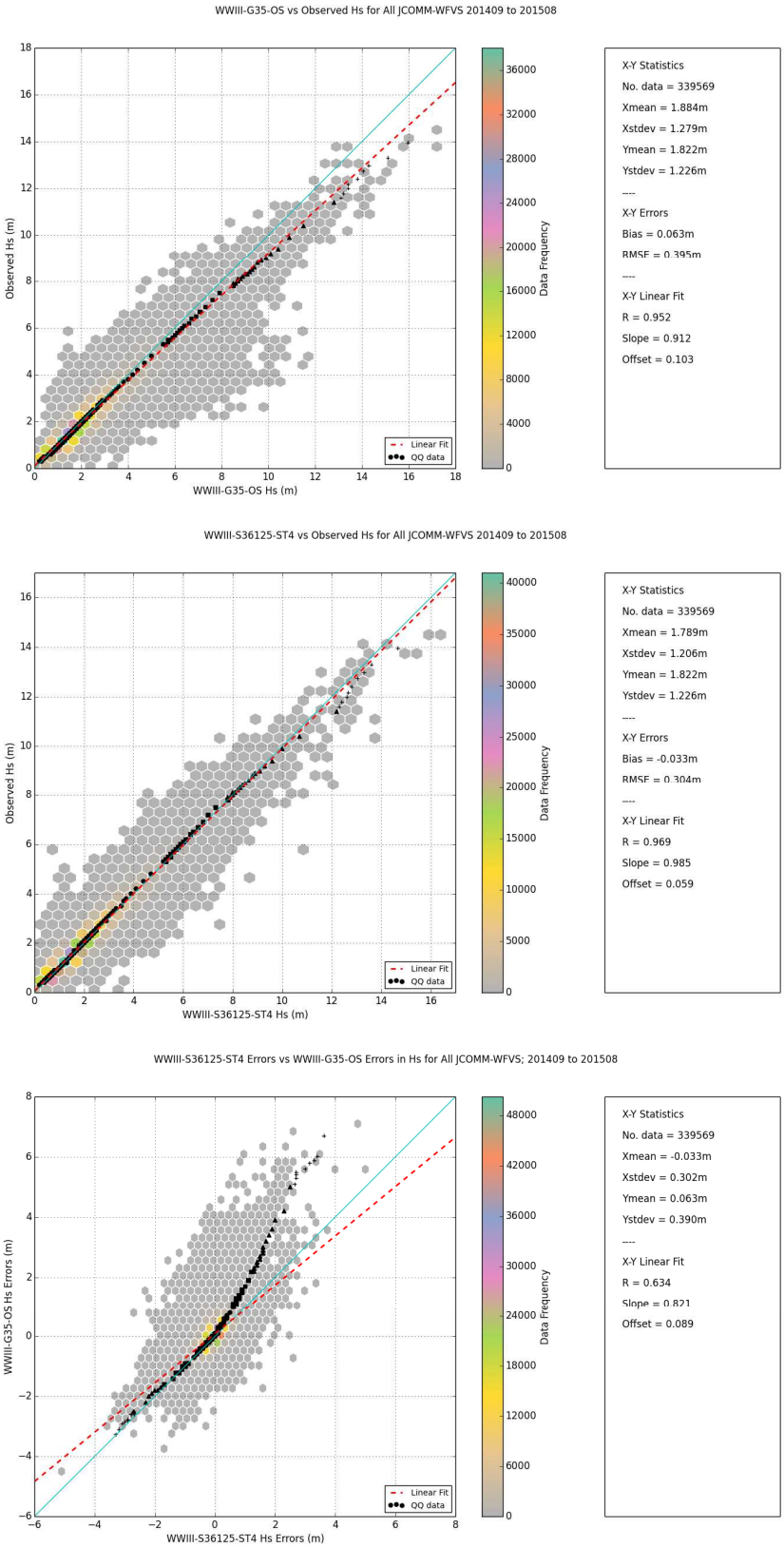

Figure 6: Significant wave height QQ and scatter data for all JCOMM-WFVS in-situ sites. Top, comparison against OS34-35 model; centre, comparison against S36125 model; bottom, comparison of OS34-35 versus S36125 errors.

Peak period is a much lower performing statistic for both models (RMSE is 24% of the background signal). In part this is due to the instability of Tp as a parameter and the potential for very large errors to occur in the presence of multi-modal seas (for which a small variation in the energy assigned to one spectral component can lead to a large variation in the identified peak frequency). Bias in the S36125 model is slightly increased, but by less than 1% of background, whilst RMSE is reduced by 5% versus the background signal (relative change in errors of 17%). Both model standard deviation and correlation with observations are improved for Tp in the S36125 model, implying that representation of the observed signal has been improved. The error QQ distribution in Figure 7 suggests that the main benefit of the S36125 model is a reduction in the number of major under-prediction errors; these are suspected to be most likely to occur when forecasting multi-modal sea states.

Mean zero-upcrossing periods are more robustly forecast by the models (e.g. overall RMSE for S36125 is 14% of the background signal). The overall statistics and plots in Figure 8 show only a limited change between OS34-35 and S36125. The S36125 configuration improves RMSE by approximately 1% versus background, although an under-prediction bias is increased by approximately 2% compared to the OS34-35 models.

The regional breakdown in Tables 2-5 assesses whether the model changes are consistent for various sea areas around the world and highlights where performance may deviate significantly from the overall figures. In the tables, the data in the S36125 model statistics columns have been emboldened where these represent an improvement over OS34-35. For the key indicator of RMSE, an improvement in wave parameter performance is found: in all regions except for the Australian East Coast for Hs; for all regions except for the Iberian Atlantic (same performance level) for Tp; for all regions except for the Western Mediterranean for Tz. In general these improvements are aligned with a positive change in the model-observation correlation, suggesting that the timing of storm peaks and lulls is improved in the new model. The change in bias and standard deviation statistics is more mixed, but variations between the models are generally small (implying a neutral change). Overall the standard deviation statistics suggest that the S36125 wave parameters fluctuate slightly less than for the OS34-35 models, which is consistent with the reduced likelihood of major under-prediction or over-prediction errors shown in Figures 6-8.

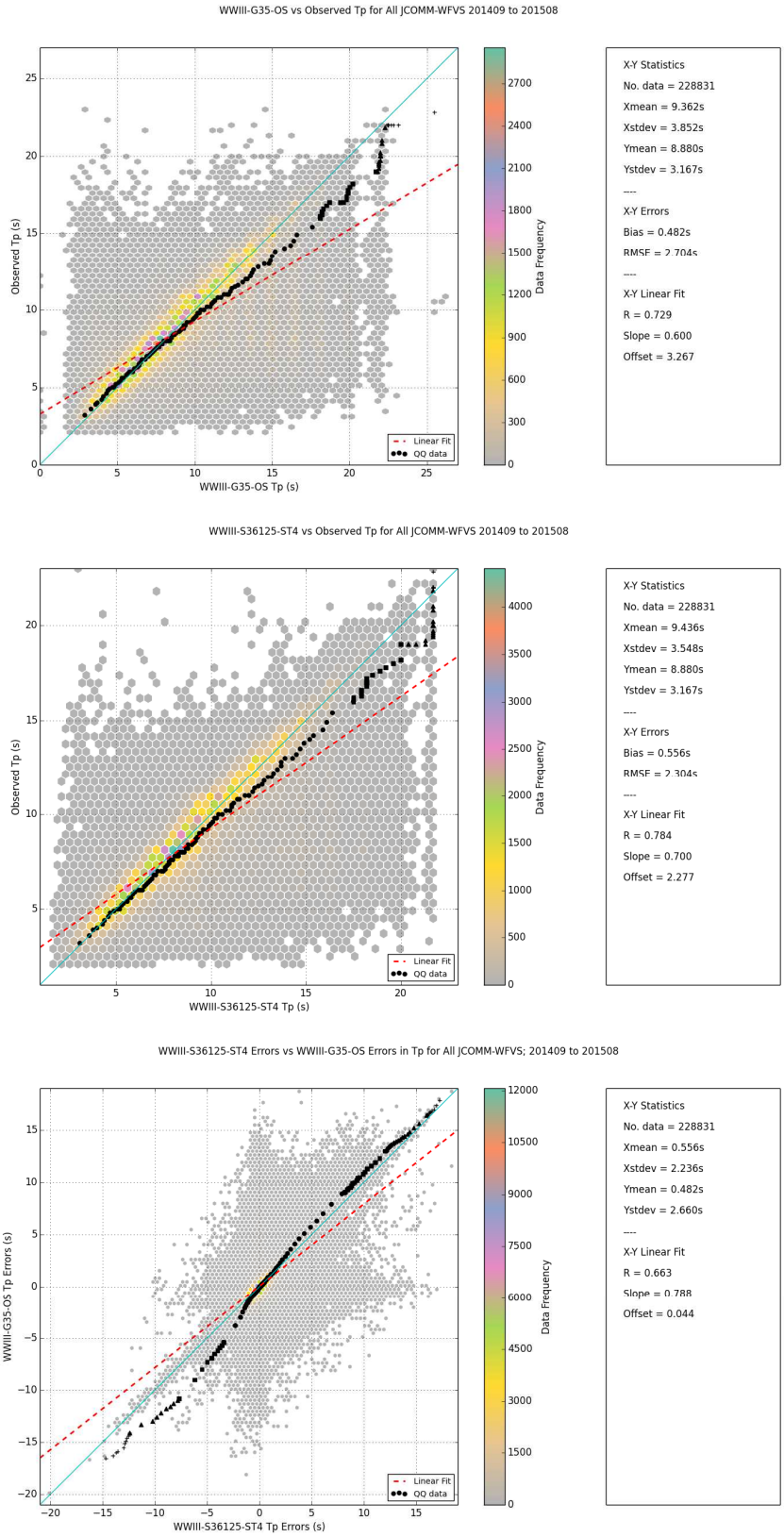

Figure 7: Peak period QQ and scatter data for all JCOMM-WFVS in-situ sites. Top, comparison against OS34-35 model; centre, comparison against S36125 model; bottom, comparison of OS34-35 versus S36125 errors.

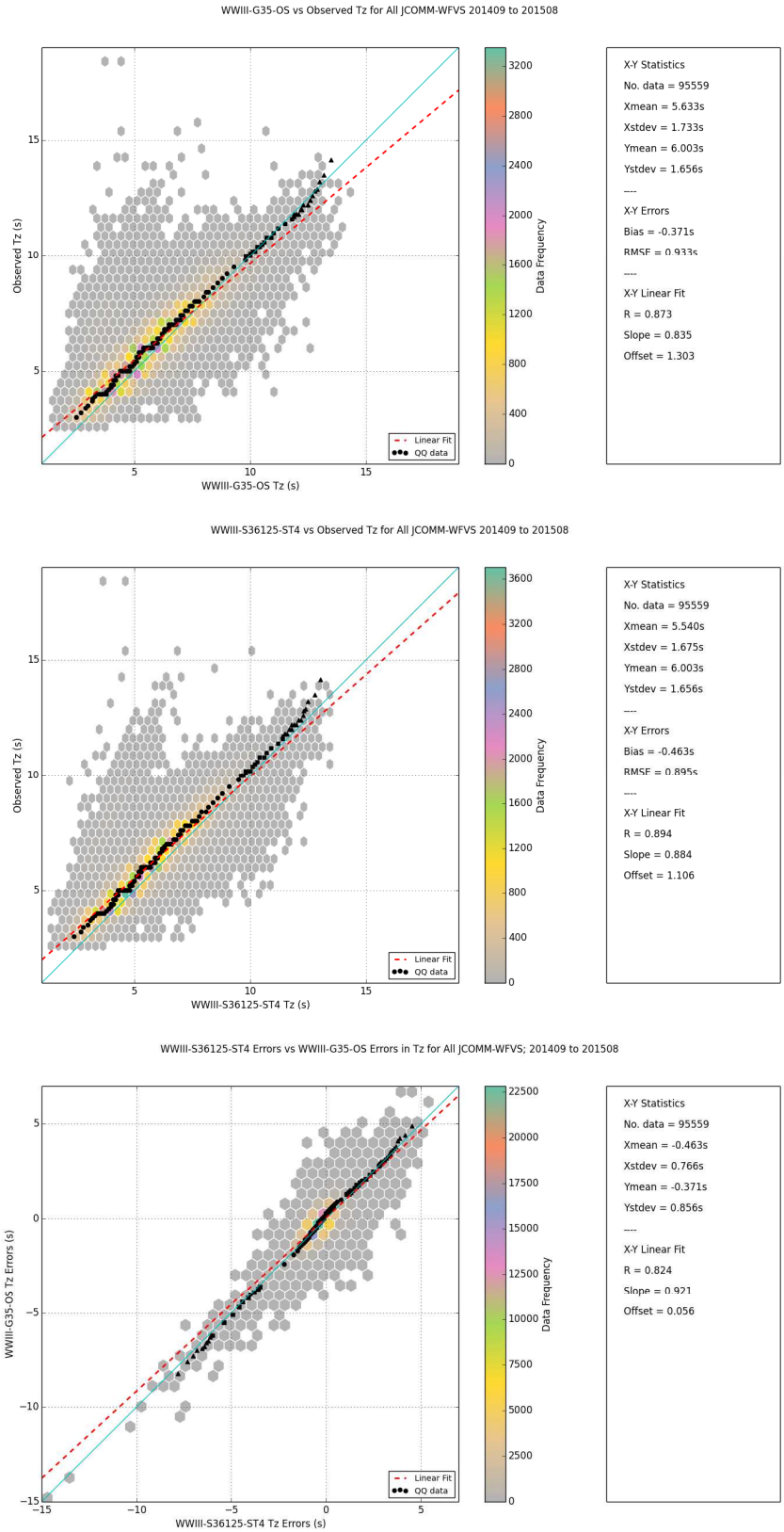

Figure 8: Mean zero-upcrossing period QQ and scatter data for all JCOMM-WFVS in-situ sites. Top, comparison against OS34-35 model; centre, comparison against S36125 model; bottom, comparison of OS34-35 versus S36125 errors.

The only major negative impact relates to Australian East Coast Hs. In this case the errors reflect a reduced ability of the S36125 model to reproduce high (4-6m Hs) wave conditions as well as the OS34-35 models, although both systems under-predict the observations quite significantly. Co-located observed and modelled wind data are not available for this region and acquisition of further wind information, needed to analyse the problem, was outside the scope of these trials. Some increase in under-prediction bias for wave heights and periods is noted for the Mediterranean but, in the case of the OS34-35 models the better bias statistic masks a tendency to under-predict at low wave heights and over-predict in storm conditions, whereas the offset in the S36125 model-observation comparison is more systematic and leads to an improvement in terms of RMSE. Regionally, the poorest performing areas are in the Mediterranean and Korea-Japan. This is consistent for all models, which may suggest causes for the errors which are additional to the choice of wave model configuration (e.g. a generic issue in the way the source terms represent wave growth in short fetches, or discrepancies in the observations post processing). Wind speed errors are notably higher in these regions (Table 4) and may also be a contributing factor. Peak period is poorly replicated in the Irish Sea; again this is a problem for all models. Inspection of the data indicates that the observed Tp in this region never exceeds 10 seconds, whilst the model will report longer period swells irregularly; the large errors in such cases contribute heavily to RMSE values. The Irish Sea is a shallow, fetch constrained body of water with strong currents and it may be that wave growth processes in such an environment are not well replicated by these models (Palmer and Saulter; 2016).

A significant positive for the S36125 model is the improvement in prediction of Hs (5% RMSE improvement against the background signal), Tp (3%) and Tz (1%) in the UK Western Approaches region. This area corresponds to the boundary between the global model and higher resolution UK waters configurations. The verification results imply that the boundary conditions provided from the global model should be significantly improved by using the S36125 configuration. The scatter and QQ plots in Figure 9 illustrate that, using Hs as a proxy, the new model is much less likely to strongly over-predict wave energy propagating toward the UK from the Atlantic during major storms (Hs values above the 90th percentile).

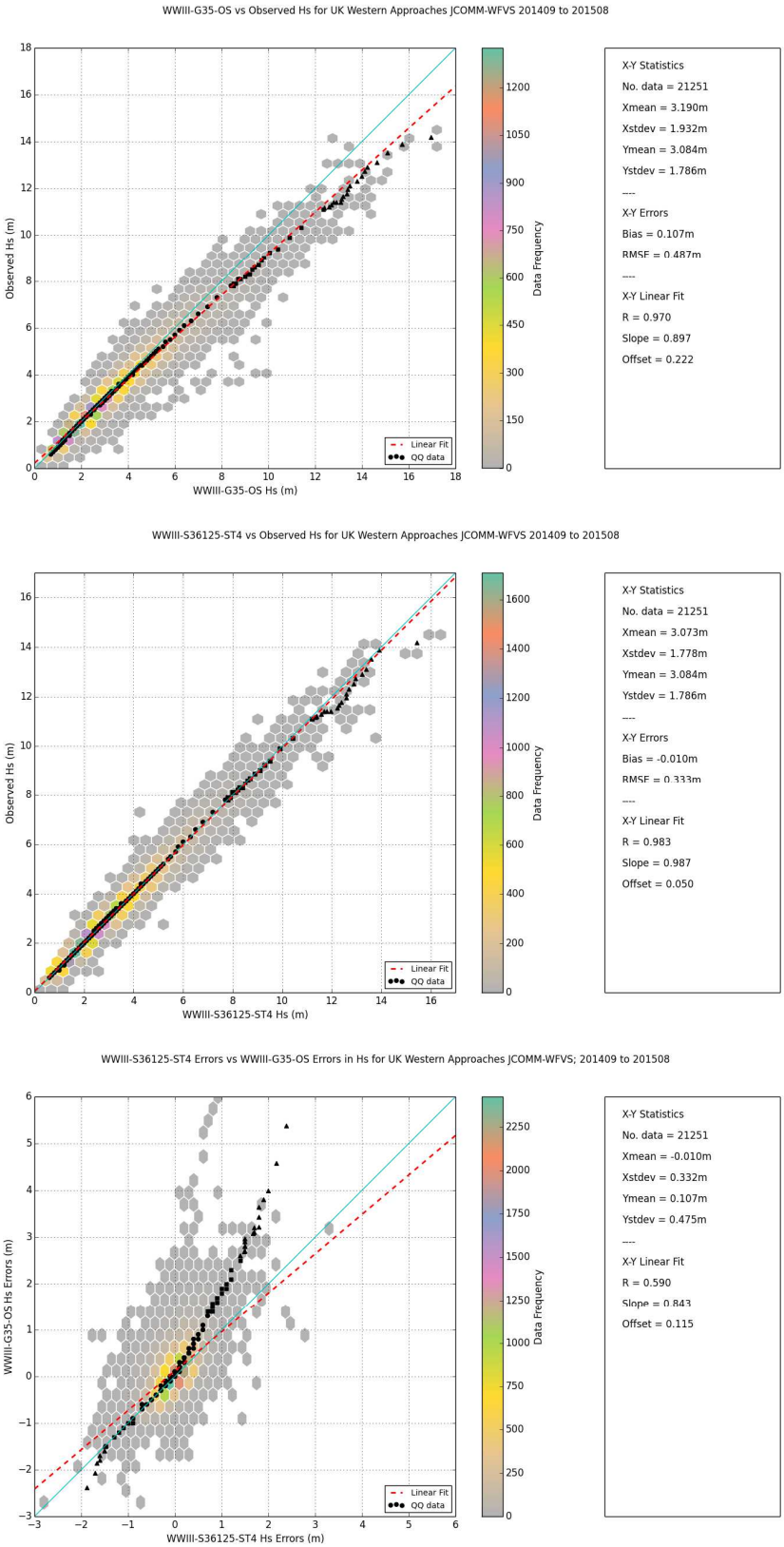

Figure 9: Significant wave height QQ and scatter data for JCOMM-WFVS in-situ sites in the UK's Western Approaches. Top, comparison against OS34-35 model; centre, comparison against S36125 model; bottom, comparison of OS34-35 versus S36125 errors.

4.3 Comparisons versus satellite altimeter

The JCOMM-WFVS data provide some measure of the model's overall performance, but lack the coverage necessary to gain a clear understanding of quality in the southern hemisphere or open ocean regions of the northern hemisphere. A spatial comparison of model versus satellite altimeter data (Figures 10-13) resolves some of these issues. The panels in each figure show statistics derived for a set of 2 degree latitude by 3 degree longitude cells covering the global oceans and seas. Figure 10 indicates that, for significant wave height, each cell uses a sample of between several hundred and several thousand model-observation match-ups. The bottom panel in Figure 10 shows mean Hs over the 1-year sample period and clearly indicates the major storm tracks and wave generating regions in the northern and southern hemisphere oceans, along with large areas of ocean influenced by both swells from those storms and trade winds in the Indian Ocean, North and South Pacific.

Figure 11 shows normalised RMSE, bias and standard deviation for the S36125 wave model Hs. In the regions with the strongest wind inputs (see lower panel in Figure 12), RMSE is particularly low, being order 10-15% of the observed root mean squared Hs. Normalised errors increase in more swell dominated areas of the open ocean (e.g. the doldrums, RMSE of 15%) and around coasts and enclosed seas (e.g. Mediterranean, Gulf of Mexico, Southeast Asia; RMSE of 20-25% or more). Cross referencing against similar plots presented in Ardhuin et al. (2010) and Saulter (2015) suggests that the results are consistent with previous studies and an improvement on the model applied at OS35 (the TS3M configuration in Saulter, 2015). Normalised bias and standard deviation statistics indicate that the model's sample climate mean and variability generally falls within 5% of the observed values for Hs. Exceptions for bias are found close to the ice edge and in coastal seas, whilst standard deviation of the model is significantly lower than that for the observations in the tropics. The areas with the poorest bias scores tie in closely with regions where RMSE is large, implying that the underlying bias may make a significant contribution to the overall errors.

No work has been undertaken at this stage to determine to what extent the increase in errors in these regions might be related to either the quality of the global atmospheric model wind field or the quality of the altimeter data close to land. The global pattern of Hs statistics are not fully consistent with the spatial distribution of statistics for Ws (Figure 13), although there are a number of exceptions. For example, both Ws and Hs

RMSE errors are notably worse in the Mediterranean, Gulf of Mexico and Southeast Asia than in the open oceans. Patterns of standard deviation suggest that the wave model damps some of the variability imparted to it via the wind forcing (e.g. in the Southern Ocean, normalised Ws standard deviation is over-predicted by the model, whereas the relationship is close to 1 for Hs). Ws bias statistics show a general under-prediction, whereas Hs is mostly over-predicted, suggesting that the wave source terms also lead to some systematic compensation for the wind inputs. However, results for the altimeter winds somewhat contradict the in-situ validation (Figure 5), which shows a small positive bias in the modelled winds and a systematic over-prediction of upper tail wind speeds. On the other hand, the consistencies between large biases and RMSEs for Hs in near-coastal zones may indicate some systematic discrepancy between observation and model which is not found in the open ocean.

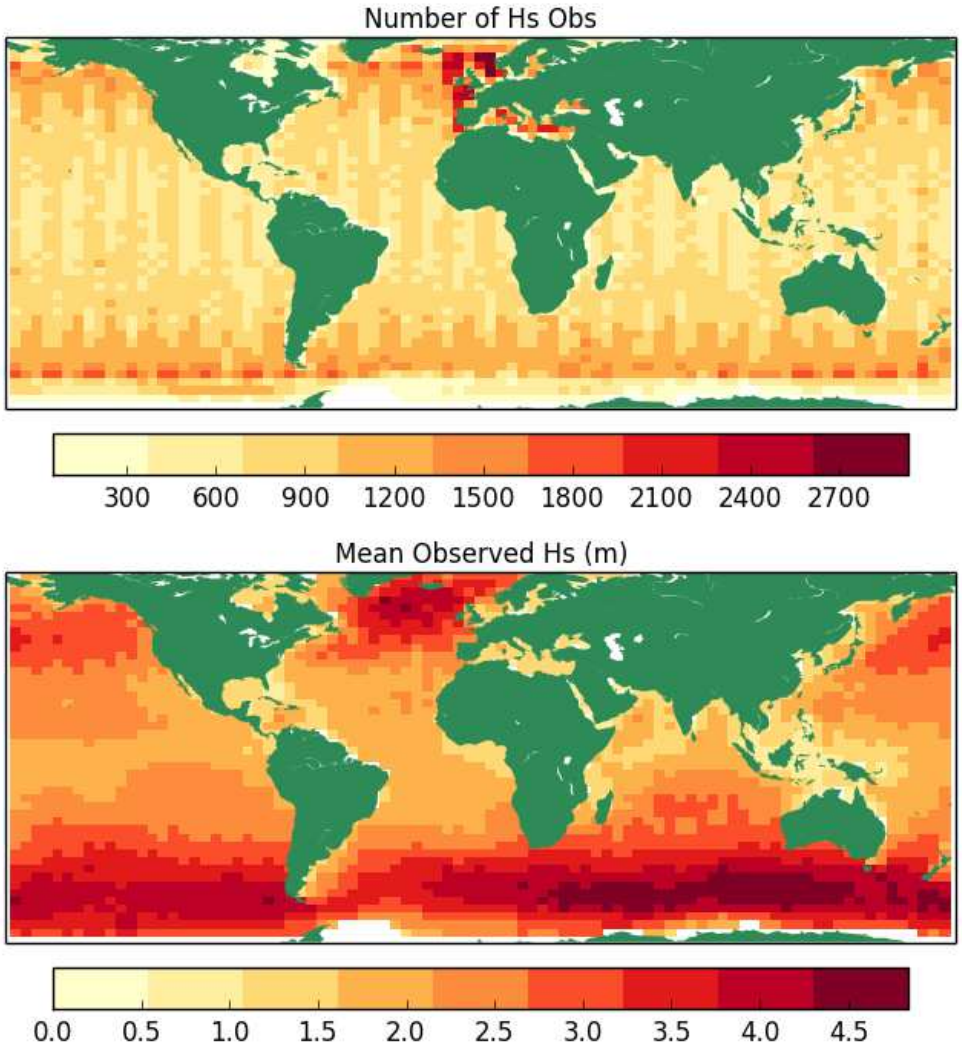

Figure 10: Observation count and observed mean significant wave height from S36125 model comparison with Cersat merged satellite altimeter dataset

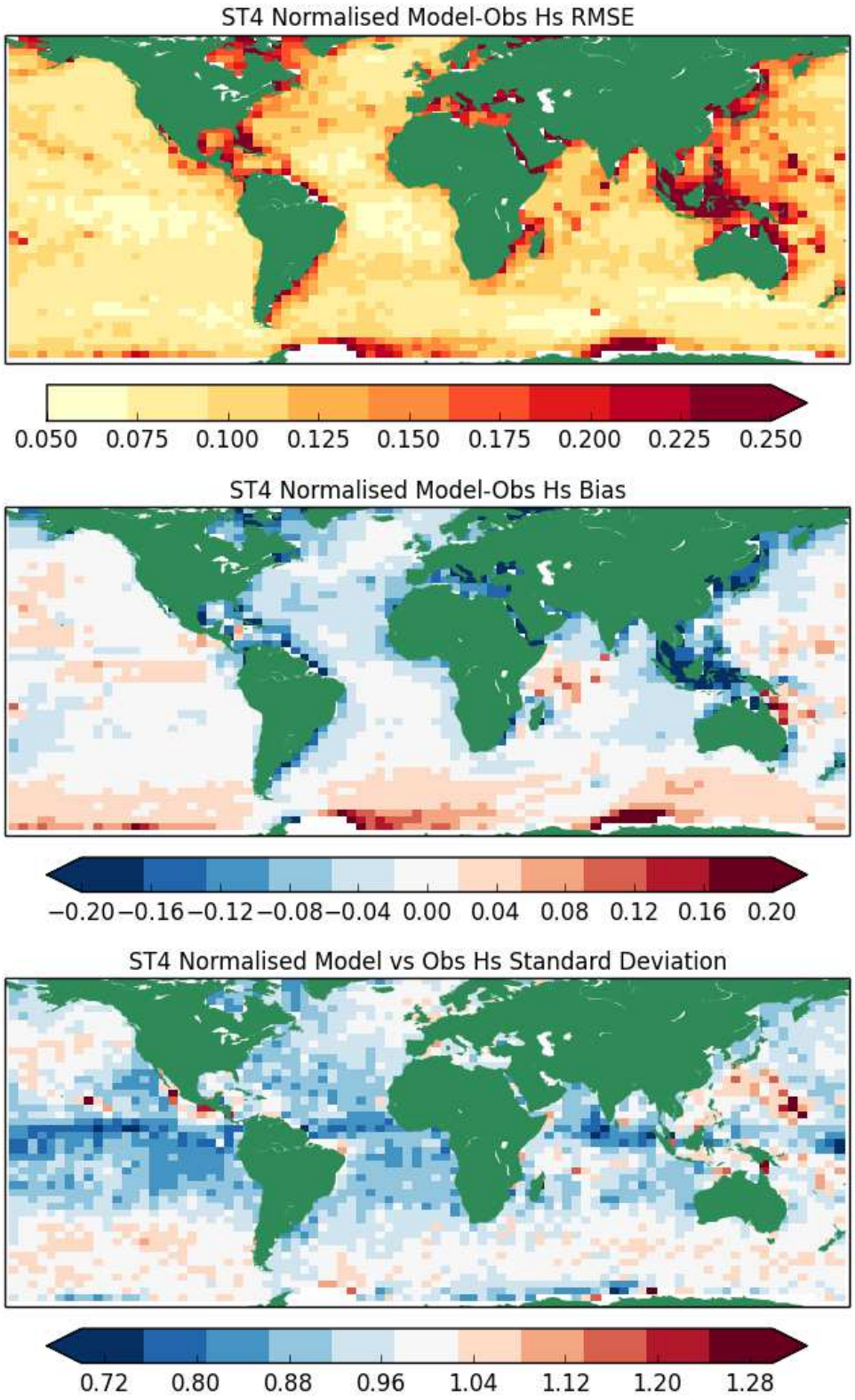

Figure 11: Normalised S36125 model-observation root mean squared error, bias and standard deviation from model significant wave height comparison with Cersat merged satellite altimeter dataset

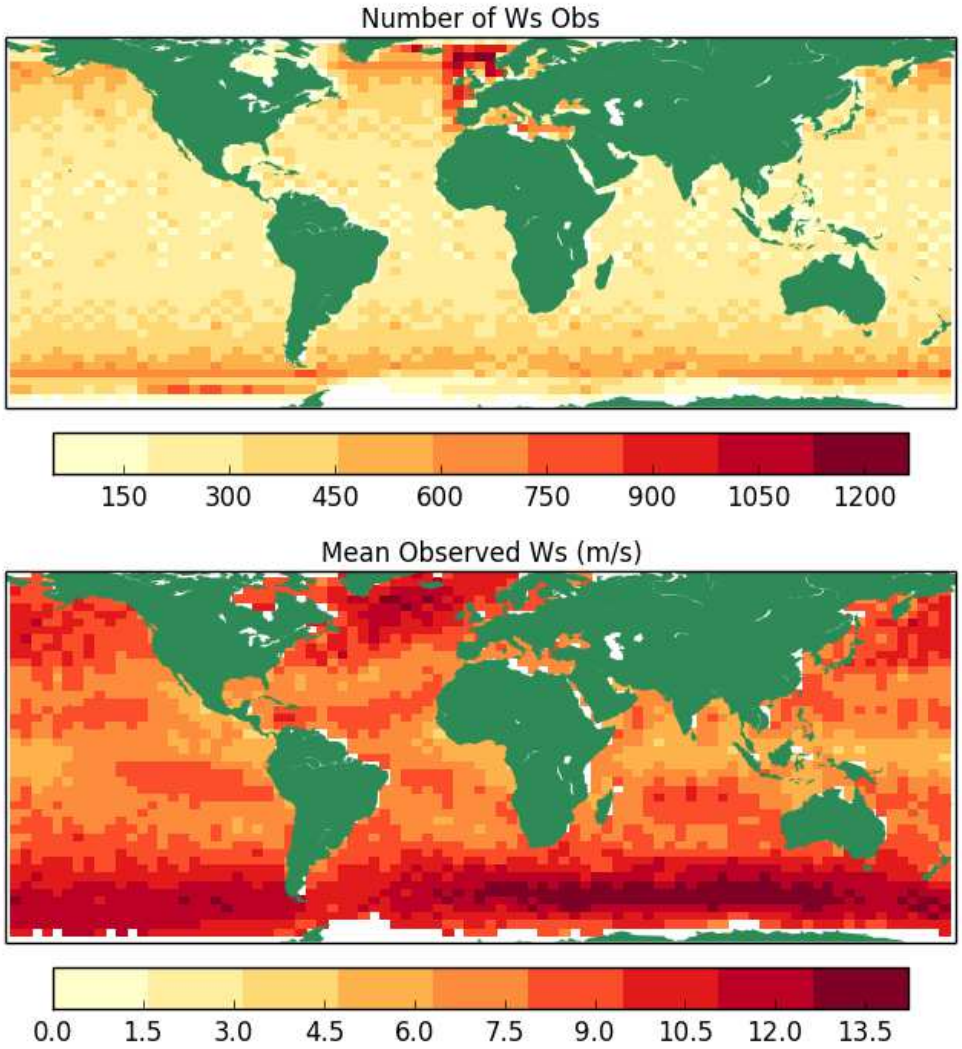

Figure 12: Observation count and observed mean wind speed from S36125 model comparison with Cersat merged satellite altimeter dataset

Scatter data for the comparison between S36125 model and altimeter wind speed and significant wave height for the Northeast Atlantic (using a domain covering 35°W to 5°E and 48°N to 74°N) are presented in Figure 14. This is a region of specific interest, which covers the area of the Atlantic designated for Met Office forecasting responsibility under Metarea I (see http://weather.gmdss.org/I.html) and also represents a large part of the storm track influencing wave energy incident to the UK. Hs RMSE is close to 10% of the observed signal, bias is less than 3% of the observed mean and the QQ data show an excellent 1:1 relationship throughout the data range. The QQ relationship for Hs follows a more linear profile than that for Ws, which under-predicts the altimeter observation for

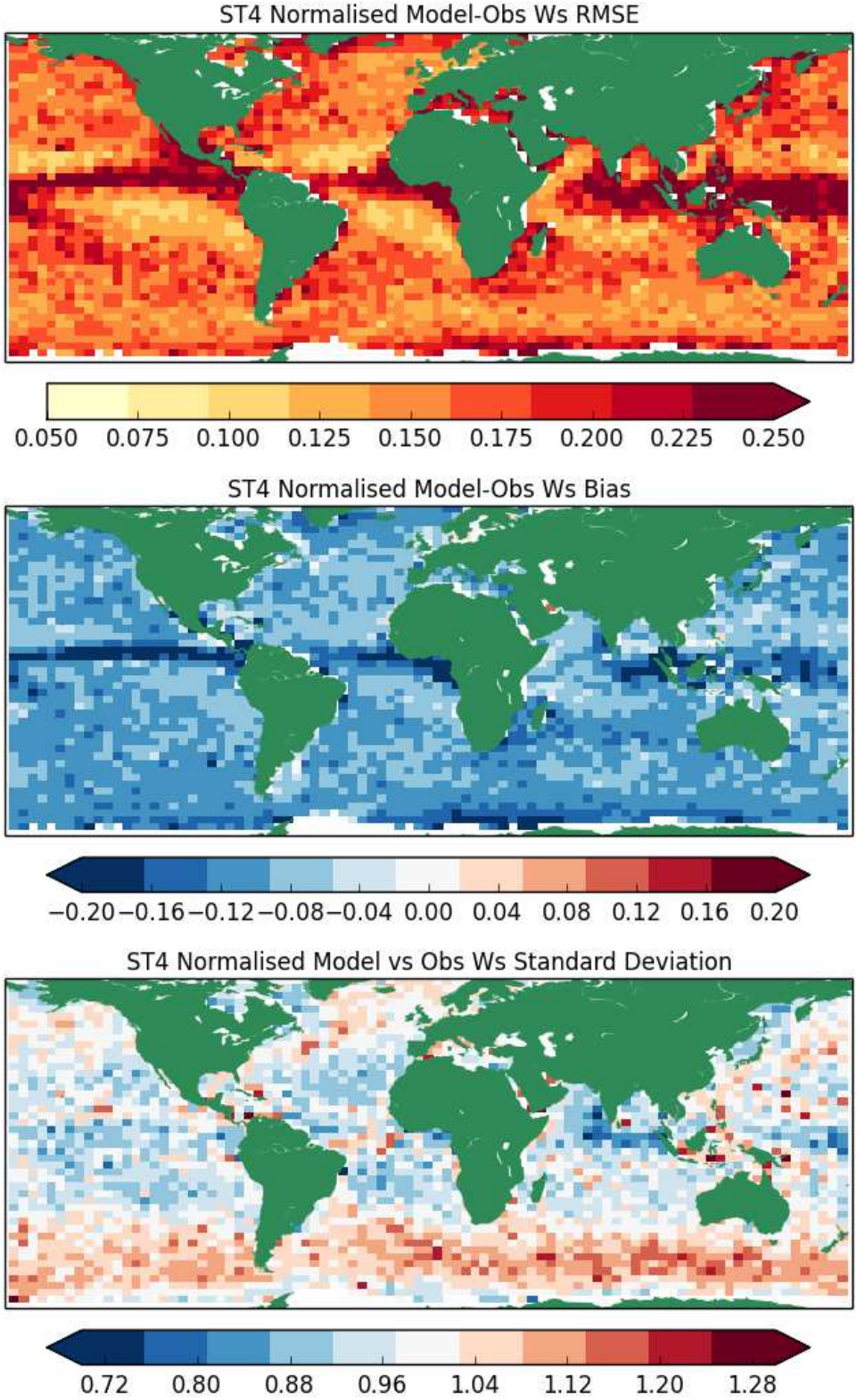

Figure 13: Normalised S36125 model-observation root mean squared error, bias and standard deviation from model wind speed comparison with Cersat merged satellite altimeter dataset

wind speeds up to 20m/s and over-predicts thereafter (above the 99th percentile). It is noted that the QQ relationship for Ws in Figure 5 is more linear, and that a further exploration of how the in-situ and altimeter observation wind speed datasets relate to each other is required as an item of further work.

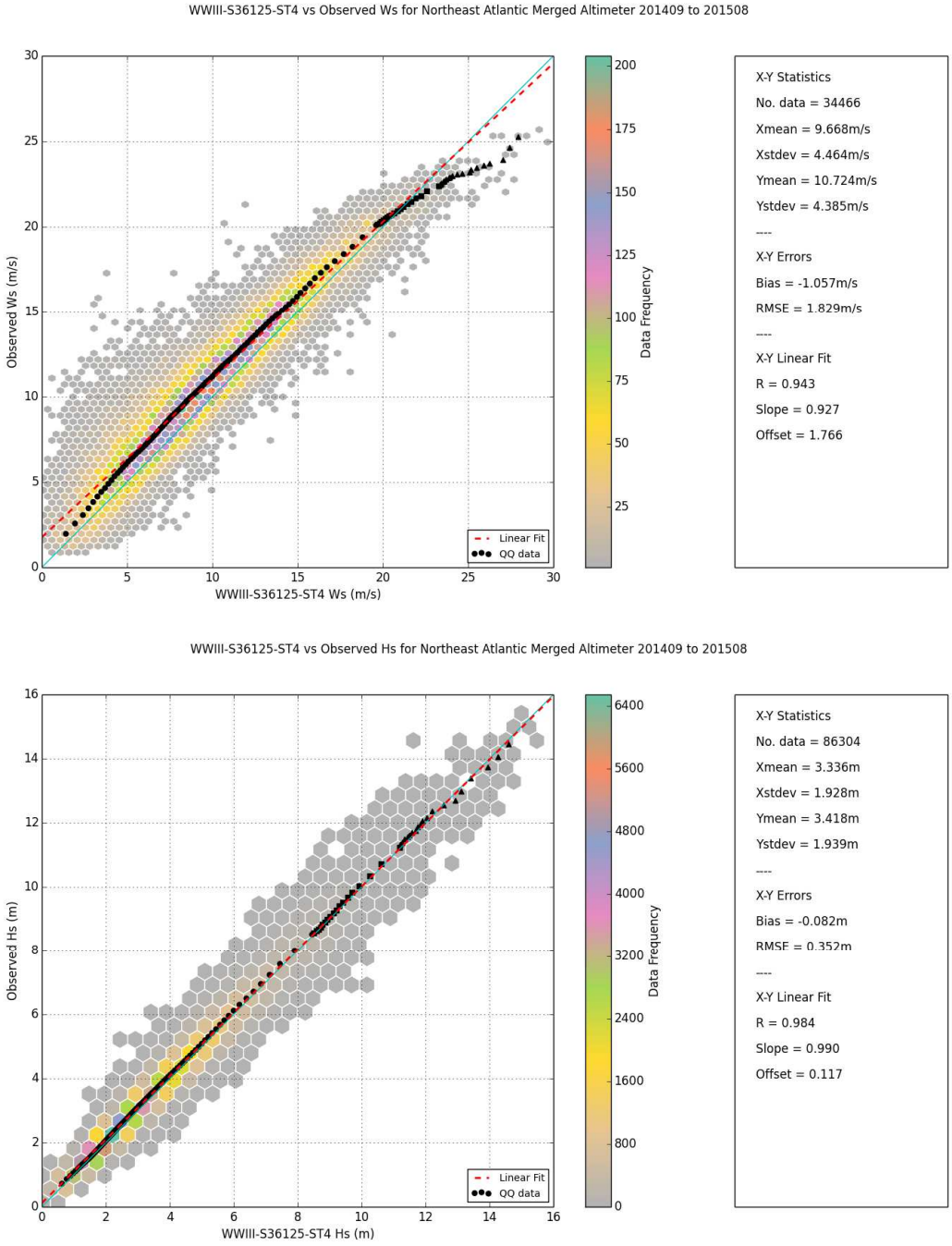

Figure 14. Wind speed (top panel) and significant wave height (bottom panel) QQ and scatter data for S36125 model versus Cersat merged altimeter product in the Northeast Atlantic.

4.4 In-situ comparisons versus OS34-35 European wave model

One of the purposes of using a multi-resolution global model is to reduce the requirement for maintaining multiple regional configurations. In this case, the 12-6-3km European zone in the S36125 configuration has a significant overlap with the (8km resolved) operational Euro8 model used by the Met Office to generate forecasts from days 3-5 in UK waters and days 1-5 elsewhere in Europe. The Euro8 model is configured based on WAVEWATCH III version 3.14 (Tolman, 2009), using WAM Cycle-4 source terms (Komen et al., 1994; with tuning settings following Bidlot, 2012) and UNO2 propagation (Li, 2008) with GSE alleviation following Booij and Holthuijsen (1987). Saulter (2015) provides some further configuration details.

As an initial test for whether S36125 model data could be used to replace Euro8 outputs, a regional comparison against JCOMM-WFVS observations was carried out, using the same trials period as for the OS34-35 comparison. Scatter and QQ diagrams for the wave parameters (Hs, Tp, Tz) are presented in Figures 15-17, whilst regional statistics for wind speed and wave parameters are provided in Tables 6-9. Both figures and tables follow the same format as described in Section 4.2.

The overall and regional statistics show a general improvement for S36125 Hs and a neutral impact for the period parameters. As for the OS34-35 comparison, the most obvious impact of the new configuration is a reduction in the size of over-prediction errors associated with the upper tail of the Hs distribution (Figure 15). Some reduction of under-prediction errors in Tp is also obtained (Figure 16). Due to the comparable resolutions of the two models and general location of the JCOMM-WFVS sites 10s of kilometres from the shore, it seems most logical that this improvement is related to the change in the WAVEWATCH III source code to version 4.18 and adopting the ST4 source terms, rather than the SMC grid scheme.

Whilst the S36125 errors are generally of the order 10-20% for Hs and Tz, the Tp errors were found to be much more variable (ranging from 8% to 39% of the observed signal). Regions with performance that was notably worse than the overall statistic are the Irish Sea and Mediterranean and, for period parameters only, the Southern North Sea and Iberian Atlantic. As was found in the OS34-35 comparison, these issues were common to both model set-ups, implying influences on the model-observation errors that are additional to the wave model configuration. The Euro8 runs were forced using the same

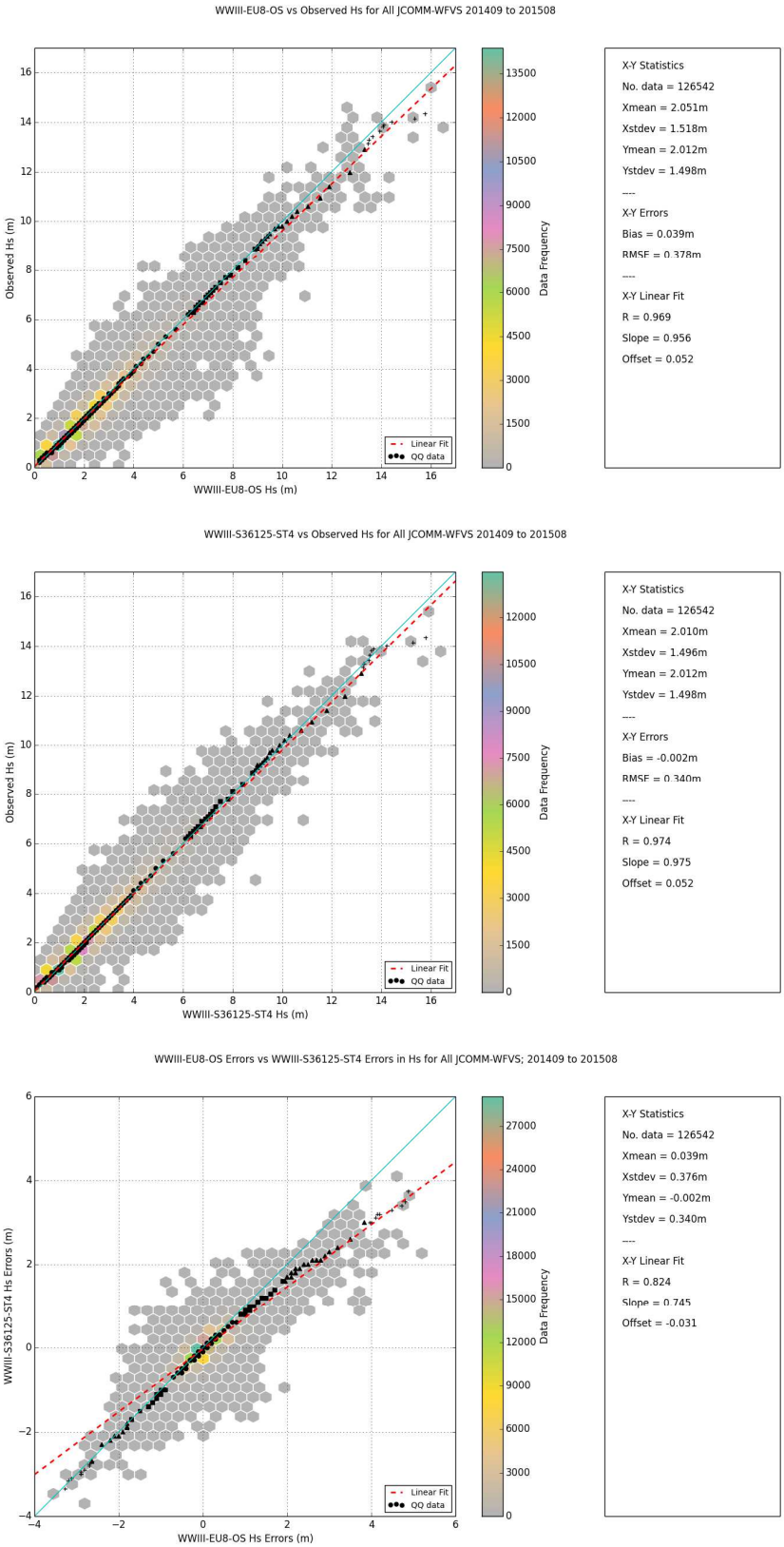

Figure 15: Significant wave height QQ and scatter data for JCOMM-WFVS in-situ sites in European wave model domain. Top, comparison against EU8-OS model; centre, comparison against S36125 model; bottom, comparison of EU8-OS versus S36125 errors.

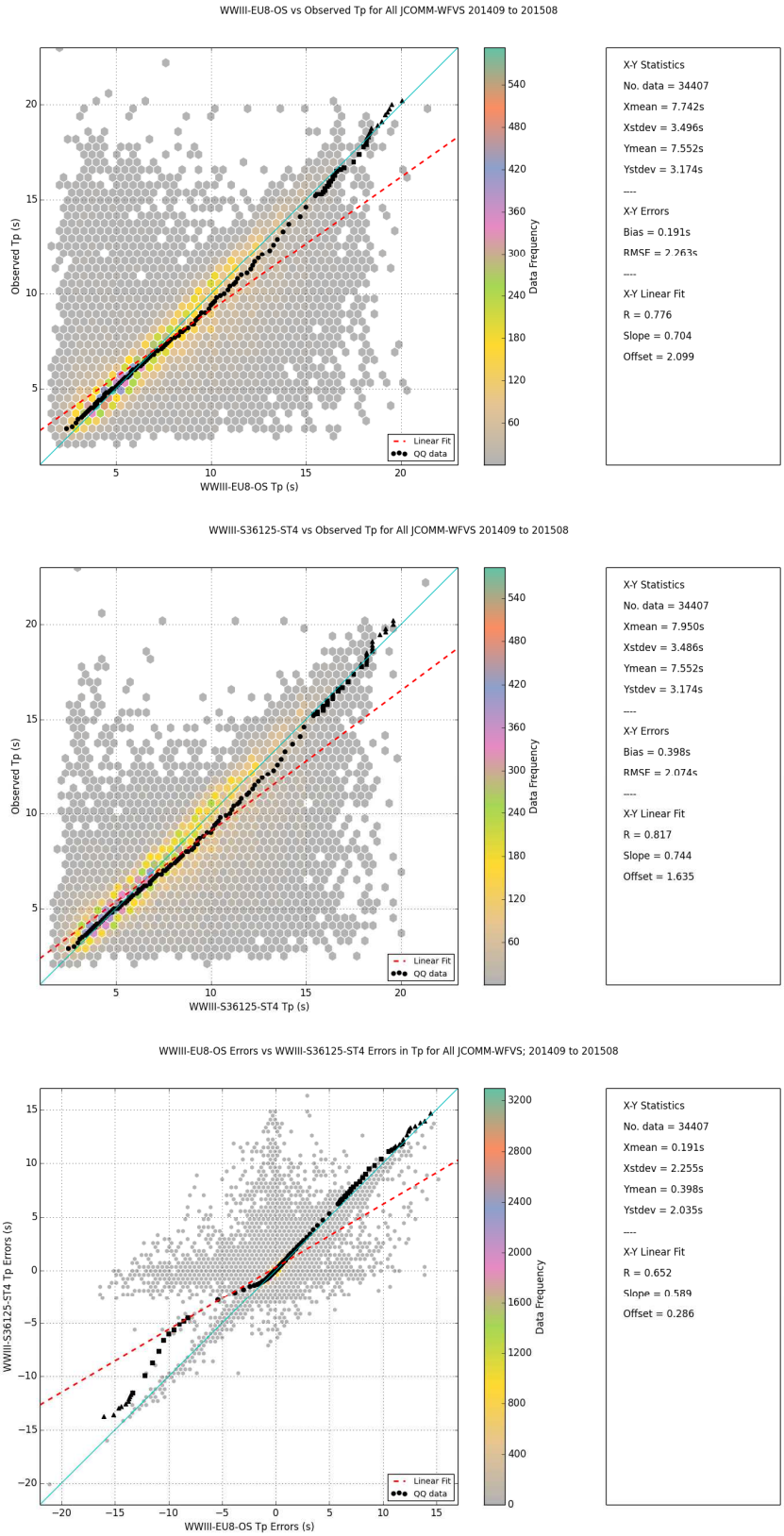

Figure 16: Peak wave period QQ and scatter data for JCOMM-WFVS in-situ sites in European wave model domain. Top, comparison against EU8-OS model; centre, comparison against S36125 model; bottom, comparison of EU8-OS versus S36125 errors.

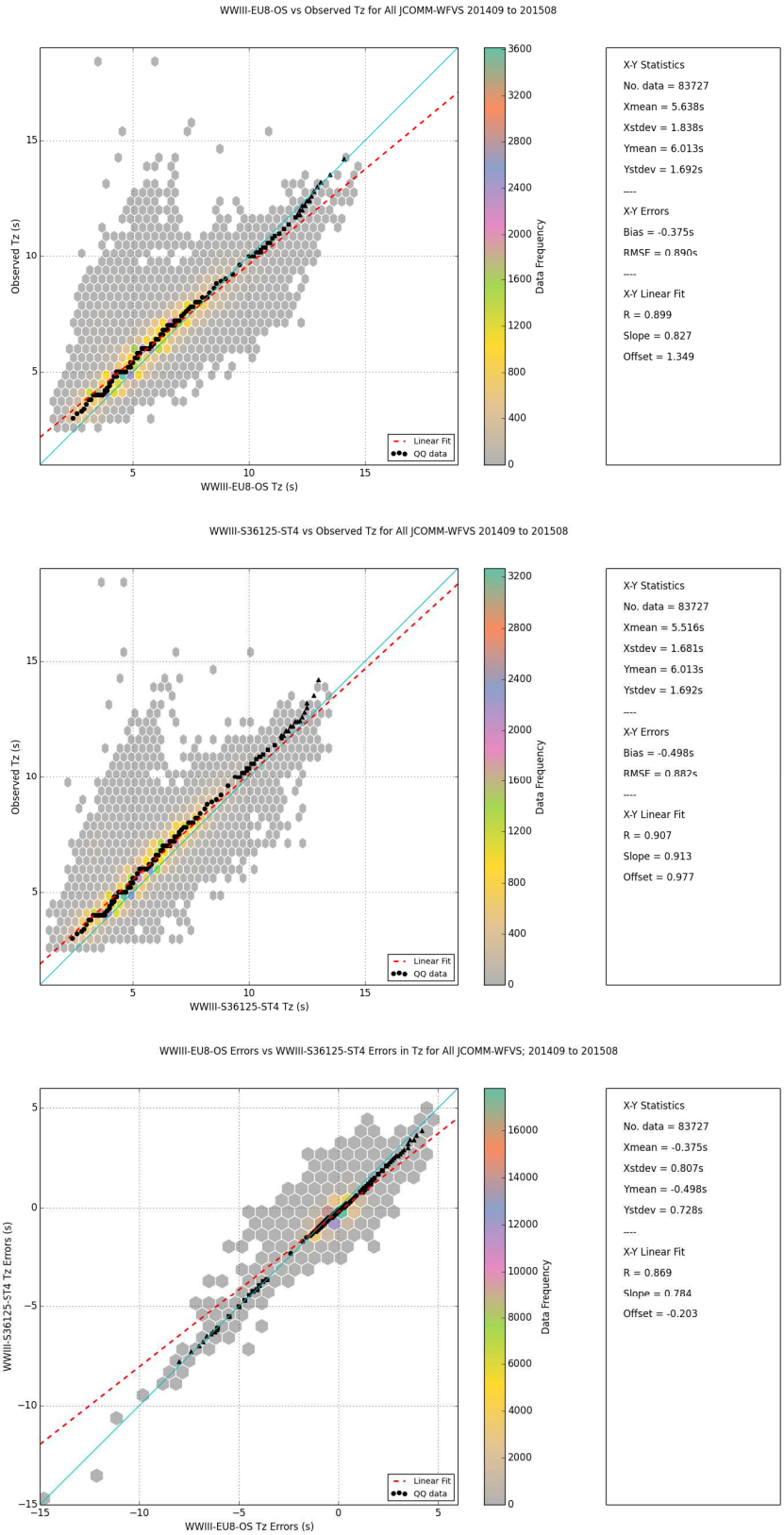

Figure 17: Mean zero-upcrossing wave period QQ and scatter data for JCOMM-WFVS in-situ sites in European wave model domain. Top, comparison against EU8-OS model; centre, comparison against S36125 model; bottom, comparison of EU8-OS versus S36125 errors.

wind speed data as for the global models, so this might be the common source of error in the Mediterranean, where normalised Ws errors are 30% or more (Table 6). Similarly, none of the models include influences of currents in the Irish Sea. In the Southern North Sea and Iberian Atlantic, visual inspection of the period data suggested that, rather than a model problem, there may be some metadata issues in the JCOMM-WFVS dataset; such that the type of period data returned by particular platforms is not correctly identified (i.e. Tp values are identified as Tz and vice-versa).

Table 6. Wind speed (Ws) statistics for European regional and sub-area JCOMM-WFVS data. Observed mean and standard deviation values are in ms^{-1}, other statistics are normalised according to the description in section 4.2.

	Observed		S36125-ST4				EU08-OS			
Region	Mean	StDev	RMSE	Bias	StDev	Corr	RMSE	Bias	StDev	Corr
All	7.76	4.03	0.18	**0.02**	1.03	0.93	0.17	0.03	1.03	0.93
Irish Sea	7.30	3.38	**0.19**	**0.10**	**1.15**	0.94	0.19	0.10	1.15	0.94
Central North Sea	8.58	4.10	0.14	**-0.01**	1.00	0.95	0.14	-0.01	1.00	0.95
Southern North Sea	7.68	3.67	0.19	**-0.03**	1.01	0.90	0.19	-0.03	1.01	0.91
Northern North Sea	8.56	4.23	0.14	0.03	1.02	0.95	0.14	0.03	1.02	0.96
UK Northwest Approache	8.89	3.90	0.16	**0.08**	1.11	0.95	0.16	0.08	1.11	0.95
UK Southwest Approache	7.91	3.55	0.16	**0.08**	**1.09**	0.94	0.16	0.08	1.09	0.95
West Mediterranean	5.67	3.87	0.26	**0.06**	**1.06**	0.91	0.26	0.08	1.07	0.91
East Mediterranean	5.57	3.07	0.33	-0.08	**1.01**	0.78	0.32	0.07	1.08	0.81
Iberian Atlantic	6.10	3.28	0.23	**0.12**	1.11	0.92	0.23	0.13	1.11	0.92

Table 7. Significant wave height (Hs) statistics for European regional and sub-area JCOMM-WFVS data. Observed mean and standard deviation values are in m, other statistics are normalised according to the description in section 4.2.

	Observed		S36125-ST4				EU08-OS			
Region	Mean	StDev	RMSE	Bias	StDev	Corr	RMSE	Bias	StDev	Corr
All	2.01	1.50	**0.14**	**0.00**	**1.00**	**0.97**	0.15	0.02	1.01	0.97
Irish Sea	1.18	0.80	**0.17**	-0.04	**1.01**	0.96	0.17	0.00	1.07	0.96
Central North Sea	2.06	1.21	**0.11**	**0.03**	**0.98**	**0.98**	0.12	0.03	1.04	0.98
Southern North Sea	1.06	0.63	**0.15**	**0.05**	**1.00**	**0.96**	0.18	0.06	1.07	0.95
Northern North Sea	2.72	1.53	**0.10**	**0.02**	0.97	**0.98**	0.11	0.03	1.01	0.98
UK Northwest Approache	3.50	1.96	**0.11**	**-0.01**	**0.99**	**0.98**	0.12	-0.02	0.99	0.97
UK Southwest Approache	2.77	1.58	**0.10**	0.00	**0.99**	**0.98**	0.11	0.00	0.98	0.97
Northeast Atlantic	2.82	1.77	**0.14**	-0.02	0.96	**0.96**	0.15	0.01	0.98	0.96
West Mediterranean	1.10	0.92	**0.18**	-0.08	**0.99**	**0.97**	0.19	-0.02	1.07	0.96
East Mediterranean	1.04	0.81	0.21	-0.14	0.94	**0.96**	0.20	-0.08	1.00	0.95
Iberian Atlantic	2.19	1.32	**0.15**	**-0.01**	**0.95**	**0.96**	0.16	0.02	0.95	0.95

Table 8. Peak wave period (Tp) statistics for European regional and sub-area JCOMM-WFVS data. Observed mean and standard deviation values are in seconds, other statistics are normalised according to the description in section 4.2.

	Observed		S36125-ST4				EU08-OS			
Region	Mean	StDev	RMSE	Bias	StDev	Corr	RMSE	Bias	StDev	Corr
All	7.55	3.17	**0.25**	0.05	**1.10**	**0.82**	0.28	0.03	1.10	0.78
Irish Sea	4.74	1.39	0.38	**0.00**	1.52	0.49	0.29	-0.07	1.30	0.65
Southern North Sea	5.65	2.08	0.31	0.06	1.17	0.69	0.29	-0.01	1.14	0.70
UK Northwest Approache	11.28	2.64	**0.09**	-0.02	0.95	**0.92**	0.11	-0.01	1.03	0.89
Northeast Atlantic	11.28	2.45	**0.08**	-0.01	**1.02**	**0.93**	0.10	0.00	1.06	0.90
West Mediterranean	5.42	1.37	**0.21**	**0.02**	**1.28**	**0.74**	0.25	0.05	1.40	0.70
East Mediterranean	5.45	1.43	**0.23**	-0.14	0.91	**0.71**	0.24	-0.12	0.97	0.65
Iberian Atlantic	8.39	2.29	**0.39**	0.32	**1.16**	**0.63**	0.41	0.32	1.24	0.61

Table 9. Mean zero-upcrossing wave period (Tp) statistics for European regional and sub-area JCOMM-WFVS data. Observed mean and standard deviation values are in seconds, other statistics are normalised according to the description in section 4.2.

	Observed		S36125-ST4				EU08-OS			
Region	**Mean**	**StDev**	**RMSE**	**Bias**	**StDev**	**Corr**	**RMSE**	**Bias**	**StDev**	**Corr**
All	6.01	1.69	**0.14**	-0.08	**0.99**	**0.91**	0.14	-0.06	1.09	0.90
Irish Sea	5.06	1.44	**0.29**	**-0.21**	**0.77**	**0.66**	0.30	-0.22	0.74	0.65
Central North Sea	5.53	1.22	**0.11**	-0.07	0.88	**0.93**	0.11	-0.06	0.99	0.91
Southern North Sea	5.50	2.02	**0.40**	**-0.27**	0.42	0.42	0.40	-0.27	0.42	0.44
Northern North Sea	6.42	1.36	0.09	-0.07	0.91	**0.95**	0.09	-0.03	1.06	0.93
UK Northwest Approache	7.33	1.59	0.09	-0.06	**0.95**	**0.95**	0.09	-0.04	1.07	0.93
UK Southwest Approache	6.92	1.57	**0.10**	-0.06	**1.01**	**0.95**	0.10	-0.05	1.13	0.94
Northeast Atlantic	6.57	1.58	0.13	-0.09	**0.99**	**0.92**	0.13	-0.06	1.14	0.91
West Mediterranean	4.28	1.01	0.17	-0.13	**1.04**	0.88	0.16	-0.10	1.18	0.88
East Mediterranean	4.35	0.89	0.17	-0.14	**1.12**	**0.89**	0.17	-0.13	1.18	0.88
Iberian Atlantic	6.94	1.78	**0.09**	-0.04	**1.06**	**0.95**	0.10	-0.03	1.14	0.94

5. Summary and discussion

The November 2016 update to the Met Office global wave model comprises three elements: a change of the background model software to use WAVEWATCH III version 4.18 (with minor amendments for compatibility with Met Office systems and forecasting processes); adoption of a spherical multiple-cell (SMC) grid with four tiers of cell refinement at 25, 12, 6 and 3km; and use of the WAVEWATCH III ST4 source terms following Ardhuin et al. (2010, with minor tuning adjustments for compatibility with Met Office wind forecast data).

In addition to improving accuracy by better representing coastlines and island chains within a coarser scaled open ocean grid, the motivation for adopting the multi-resolution SMC grid is to reduce complexity and gain efficiencies in the Met Office operational wave forecast modelling suite. Complexity is reduced by having a single configuration that will be able to forecast waves in both open ocean and shelf seas waters anywhere in the world with a reasonable degree of accuracy. The refined coastal resolution in this model is a significant step in achieving this. Efficiencies will be gained by reducing the need to have additional meso-scale or higher resolution configurations in the suite and computational cost reductions associated with the model's cell refinement scheme. The ready availability of coastal forecast points across the whole globe should allow forecasters to respond rapidly to requests for wave forecasts in new locations, with a reduced need to intervene on the model guidance compared to a coarsely resolved regular grid global model.

The new model configuration (denoted S36125) has been trialled for a period of 1 year (August 2014 to July 2015) and verified against in-situ and satellite altimeter

observations. Comparisons were also made with data from global and Euro8 wave model configurations run operationally during this period. The trials indicate a significant improvement in the global model's ability to predict observed wave conditions under analysed wind forcing. For example, S36125 root mean squared error scores were approximately 5% better than those of the operational model for significant wave height (when normalised using the observed signal). Globally, RMSE values for both significant wave height and mean zero-up crossing period are 10-20% of the observed conditions. These can be contrasted with global and regional estimates of observational error (8-10%) which have been made in studies such as Janssen et al. (2007) and Palmer and Saulter (2014). These figures suggest that overall model hindcast skill is within a few percent of the achievable verification baseline (i.e. a point at which observation errors constrain our ability to quantify model improvements against an 'observed truth').

Regionally, the S36125 model was found to perform better than the global operational model for nearly all the sea areas assessed and also produced comparable, or improved, verification when compared to the European regional (Euro8) wave model. The majority of this improvement appears to be related to the S36125 model producing fewer forecast 'busts'; particularly in terms of over-prediction of large wave heights. Whilst some model improvement is attributed to the grid scheme, this particular characteristic of the model is principally related to the update in the wave model version and change in the source term scheme.

The study for this report has concentrated solely on testing the hypotheses that a) the S36125 model is of suitable quality to enable an upgrade of the Met Office global operational wave forecast model; and b) that the model can generate data of sufficient quality to replace outputs from the operational European regional model. The verification presented here has proven that the new model can fulfil both these functions, but also highlights areas for further investigation. For example, a number of regions were identified where all models performed significantly worse than the overall verification. This common behaviour may suggest additional issues related to forcing data (for example degraded wind speed verification in the Mediterranean), wave model process representation (e.g. short fetch wave growth, non-inclusion of currents) or issues with the observation quality control procedures (e.g. period metadata for Southern North Sea platforms). The study also focuses on standard observation datasets which are valid tens of kilometres or more from the coast. In the long run, the ability of a multi-resolution SMC model to represent observations made in the coastal

zone at scales of a few kilometres from shore needs to be quantifiably demonstrated beyond the promising initial study carried out by Li and Saulter (2014).

6. References

Ardhuin, F., E. Rogers, A.V. Babanin, J.-F. Filipot, R. Magne, A. Roland, A. Van der Westhuysen, P. Queffeulou, J.-M. Lefevre, L. Aouf and F. Collard, 2010: Semi-empirical dissipation source functions for wind-wave models. Part I: definition, calibration and validation. J. Phys. Oceanogr., 40 (9), 1917–1941.

Bidlot, J.-R., 2012: Present status of wave forecasting at E.C.W.M.F. In Proc. ECMWF Workshop on Ocean Waves, Reading, 2012, p1-15.

Bidlot, J.-R., J.-G. Li, P. Wittmann, M. Faucher, H. Chen, J.-M, Lefevre,T. Bruns, D. Greenslade, F. Ardhuin, N. Kohno, S. Park and M. Gomez, 2007: Inter-Comparison of Operational Wave Forecasting Systems. In Proc. 10th International Workshop on Wave Hindcasting and Forecasting and Coastal Hazard Symposium,North Shore, Oahu, Hawaii, November 11-16, 2007.

Booij, N. and L. H. Holthuijsen, 1987: Propagation of ocean waves in discrete spectral wave models. J. Comp. Phys., 68, 307-326.

Bunney, C. and A. Saulter, 2015: An ensemble forecast system for prediction of Atlantic–UK wind waves. Ocean Modelling, July 2015, doi:10.1016/j.ocemod.2015.07.005

Hasselmann, S., K. Hasselmann, J.H. Allender, and T.P. Barnett, 1985: Computations and parameterisations of the nonlinear energy transfer in a gravity wave spectrum. Part 2: Parameterisations of the nonlinear energy transfer for application in wave models. J. Phys. Oceanogr., 15, 1378-1391.

Komen, G., L. Cavaleri, M. Donelan, K. Hasselmann, H. Hasselmann and P.A.E.M. Janssen, 1994: Dynamics and Modelling of Ocean Waves, Cambridge Univ. Press, 532pp.

Janssen, P.A.E.M., Abdalla, S., Hersbach, H. and Bidlot, J.-R., 2007. Error estimation of buoy, satellite, and model wave height data. J. Atmos. Oc. Tech., 24, 1665-1677. doi:10.1175/JTECH2069.1

Leonard-Williams, A. and A. Saulter, 2013: Comparing EVA results from analysis of 12 years of WAVEWATCH III™ and 50 years of NORA10 data. Met Office Forecasting Research Technical Report 574 http://www.metoffice.gov.uk/media/pdf/8/3/FRTR574.pdf

Li, J.-G., 2008: Upstream Non-Oscillatory (UNO) advection schemes. Monthly Weather Review, 136, 4709-4729.

Li, J.-G., 2011: Global transport on a spherical multiple-cell grid. Monthly Weather Review, 139, 1536-1555.

Li, J.-G., 2012: Propagation of ocean surface waves on a spherical multiple-cell grid. Journal of Computational Physics, 231, 8262-8277.

Li, J.-G., & A. Saulter 2014: Unified global and regional wave model on a multi-resolution grid. Ocean Dynamics, 64, 1657-1670.

Li, J.-G., 2016: Ocean surface waves in an ice-free Arctic Ocean. Ocean Dynamics, 66, 989-1004.

Mentaschi, L., G. Besio, F. Cassola and A. Mazzino, 2013: Problems in RMSE-based wave model validations, Ocean Modelling, Dec 2013, Pages 53-58, ISSN 1463-5003

Mitchell, J.A., P.E. Bett, H.M. Hanlon and A. Saulter, 2016. Investigating the impact of climate change on the UK wave power climate. Meteorologische Zeitschrift, DOI 10.1127/metz/2016/

Palmer, T. And A. Saulter, 2016: Evaluating the effects of ocean current fields on a UK regional wave model. Met Office Forecasting Research Technical Report 612. http://www.metoffice.gov.uk/media/pdf/j/i/FRTR_612_2016P.pdf

Popinet S, R.M. Gorman, G.J. Rickard and H.L. Tolman: 2010. A quadtree-adaptive spectral wave model. Ocean Model 34:36–49

Queffeulou, P., 2013: Merged altimeter data base. An update. Proceedings ESA Living Planet Symposium 2013, Edimburgh, UK, 9–13 September, ESA SP-722. Available at ftp://ftp.ifremer.fr/ifremer/cersat/products/swath/altimeters/waves/documentation/publications/ESA LivingPlanet Symposium 2013.pdf .

Rasch, P. J., 1994: Conservative shape-preserving two-dimensional transport on a spherical reduced grid. Mon. Wea. Rev., 122, 1337–1350.

Roland, A., A. Cucco, C. Ferrarin, T.-W. Hsu, J.-M. Liau, S.-H. Ou, G. Umgiesser, and U. Zanke, 2009: On the development and verification of a 2-D coupled wave-current model on unstructured meshes. J. Mar. Syst., 78, S244–S254.

Saulter, A., 2015. Assessment of WAM Cycle-4 based source terms for the Met Office global-regional wave modelling system. Met Office Forecasting Research Technical Report 598. http://www.metoffice.gov.uk/media/pdf/c/s/FRTR598.pdf

Tolman, H. L., and D. Chalikov, 1996: Source terms in a third-generation wind-wave model. J. Phys. Oceanogr, 26, 2497-2518.

Tolman , H. L, 1999: User manual and system documentation of WAVEWATCH-III version 1.18. NOAA / NWS / NCEP / OMB Technical Note 166 , 110 pp.

Tolman, H. L., 2001: Improving propagation in ocean wave models. Ocean Wave Measurement and Analysis, San Francisco, CA, B. L. Edge and J. M. Hemsley, Eds., ASCE, 507-516.

Tolman, H. L., 2002: Alleviating the garden sprinkler effect in wind wave models. Ocean Mod., 4, 269–289.

Tolman, H. L., 2008: A mosaic approach to wind wave modeling. Ocean Modelling, 25, 35-47.

Tolman, H.L., 2009: User manual and system documentation of WAVEWATCH III® version 3.14. NOAA / NWS / NCEP / MMAB Technical Note 276, 194 pp + Appendices. http://polar.ncep.noaa.gov/mmab/papers/tn276/MMAB_276.pdf

Tolman, H.L., 2014: User manual and system documentation of WAVEWATCH III® version 4.18. NOAA / NWS / NCEP / MMAB Technical Note 316, 282 pp + Appendices. http://polar.ncep.noaa.gov/waves/wavewatch/manual.v4.18.pdf

Appendix A – Locations of observations for regional verification

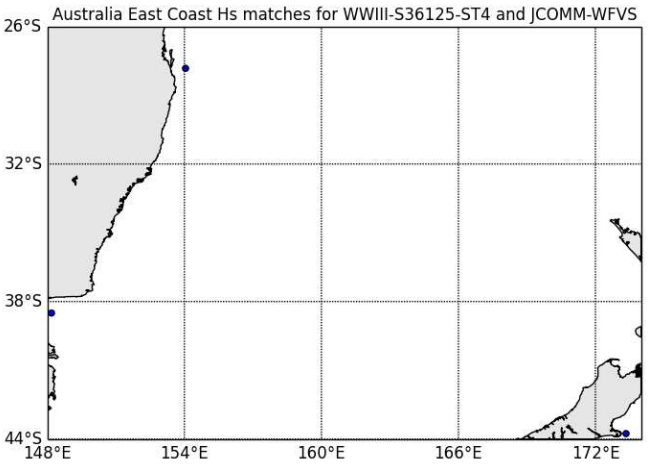

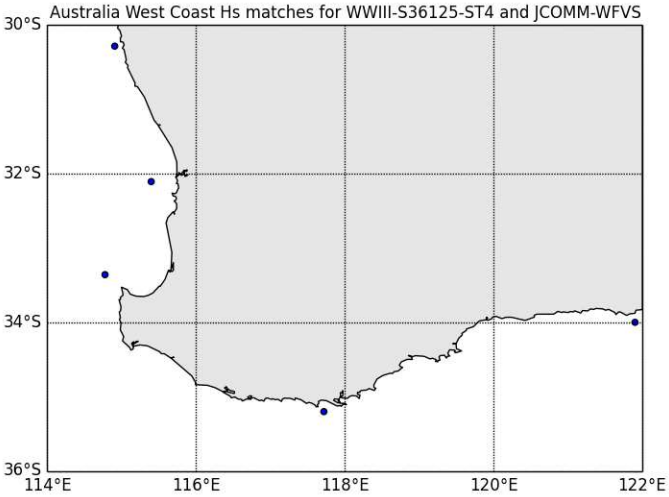

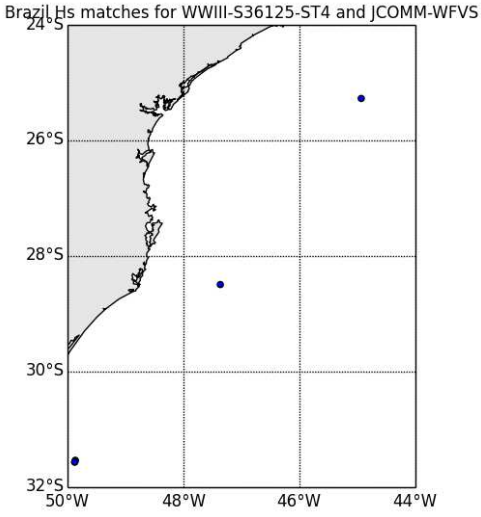

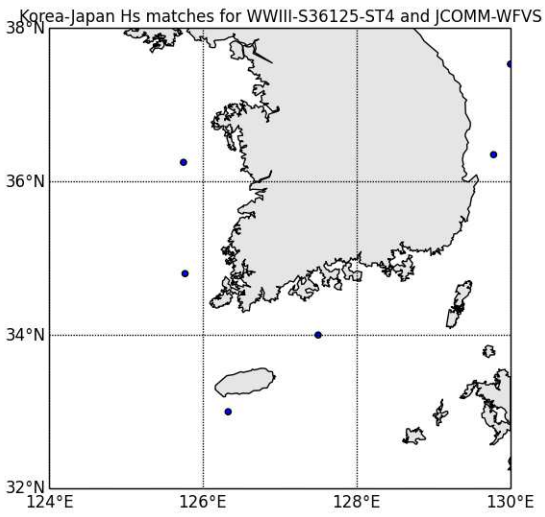

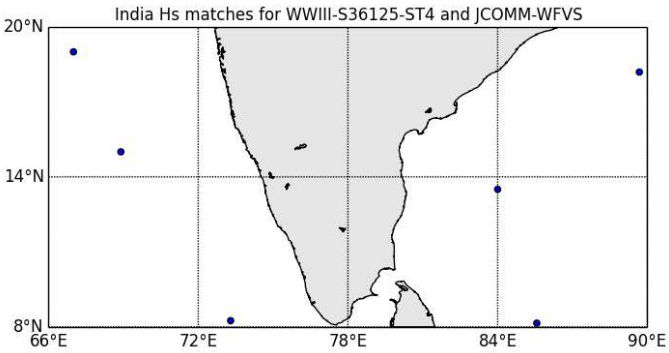

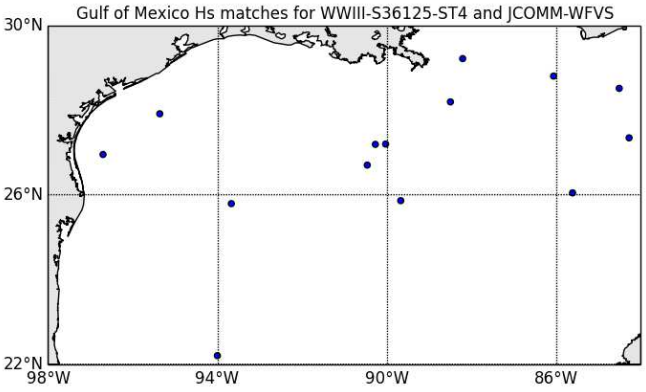

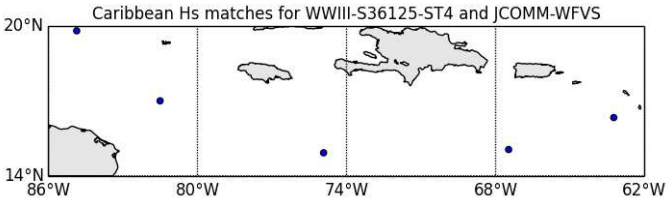

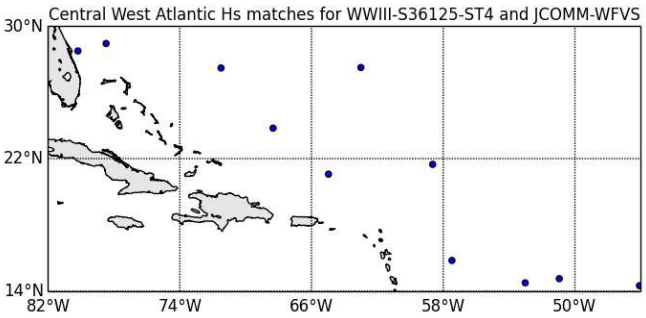

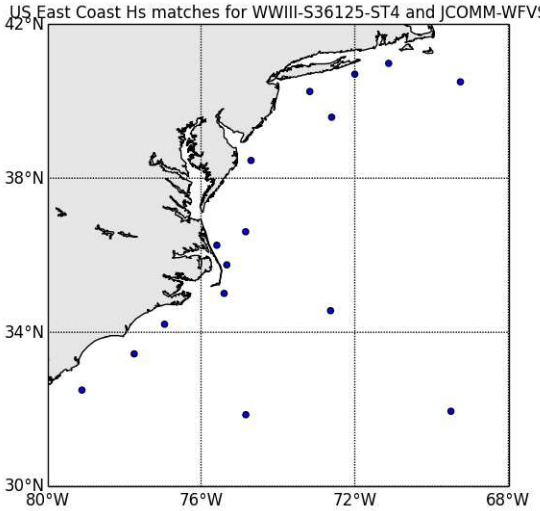

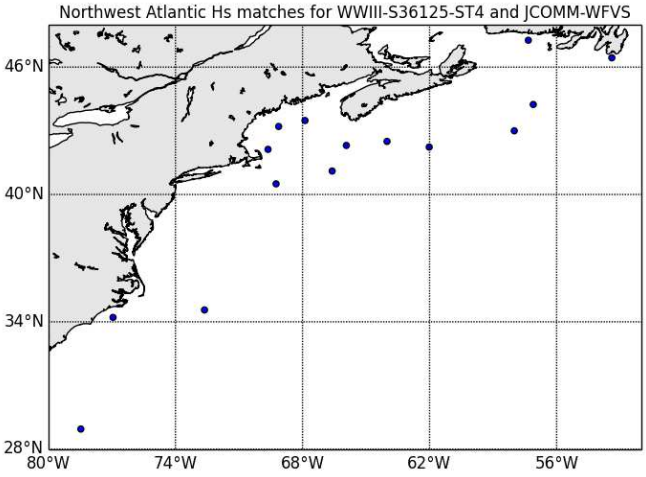

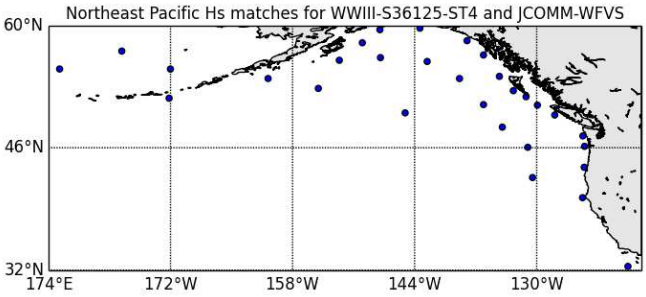

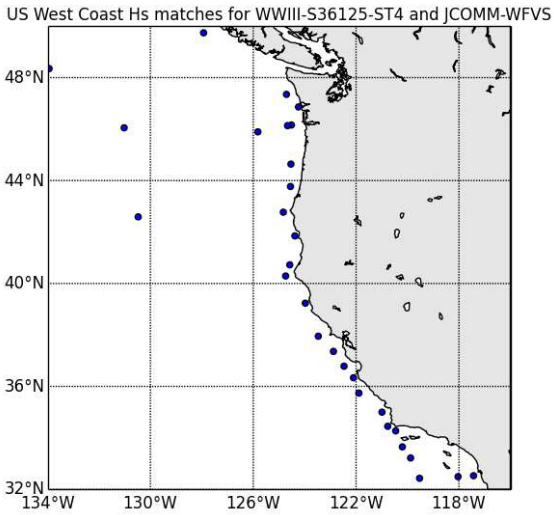

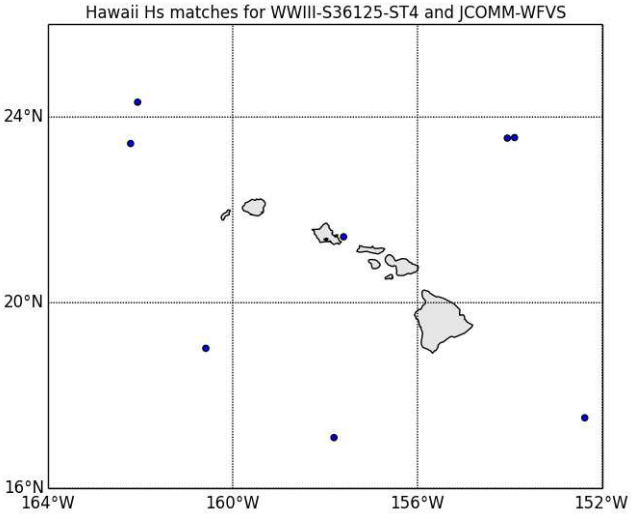

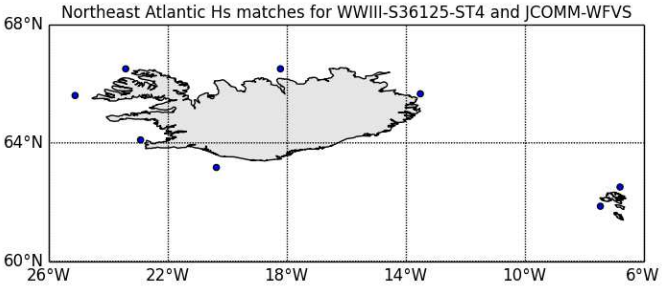

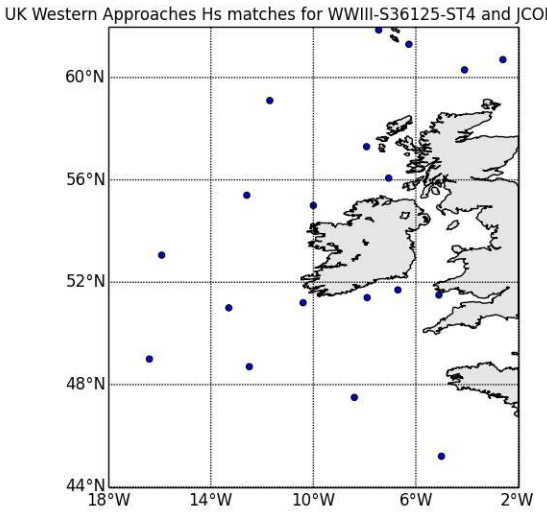

North Sea Hs matches for WWIII-S36125-ST4 and JCOMM-WFVS

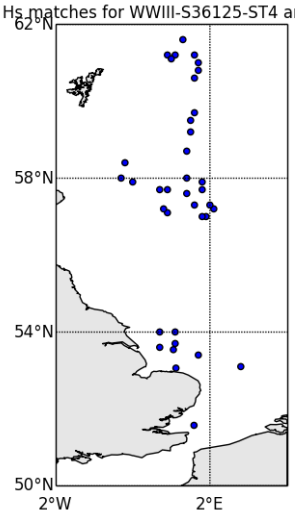

Central North Sea Hs matches for WWIII-EU8-OS and JCOMM-WFVS

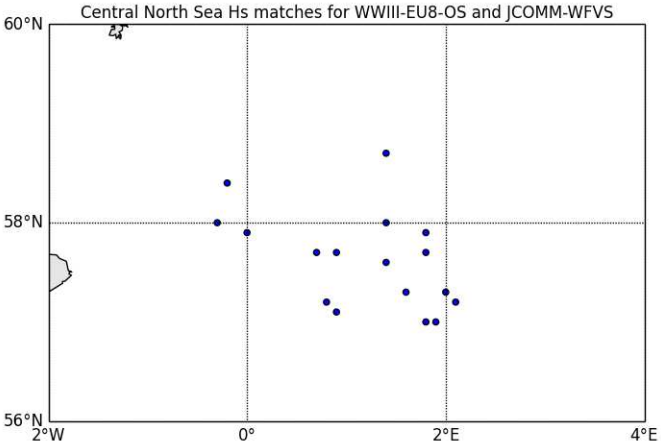

Northern North Sea Hs matches for WWIII-EU8-OS and JCOMM-WFVS

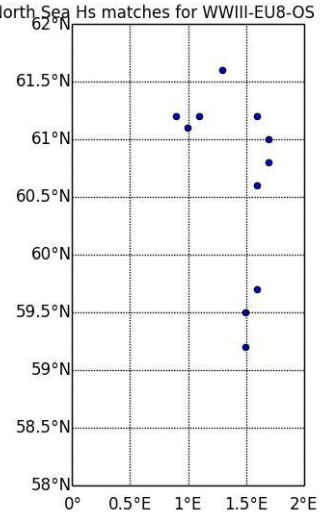

Southern North Sea Hs matches for WWIII-EU8-OS and JCOMM-WFVS

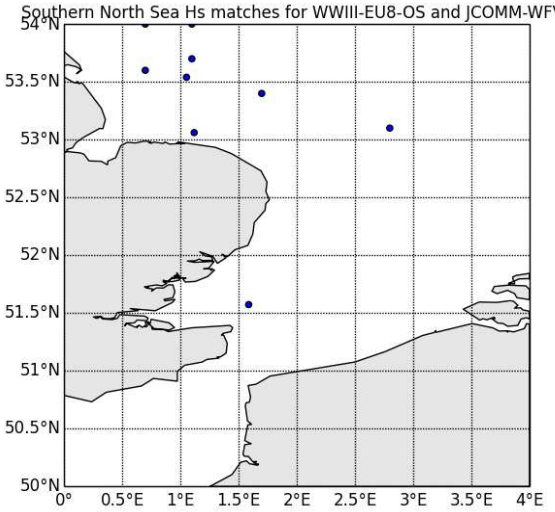

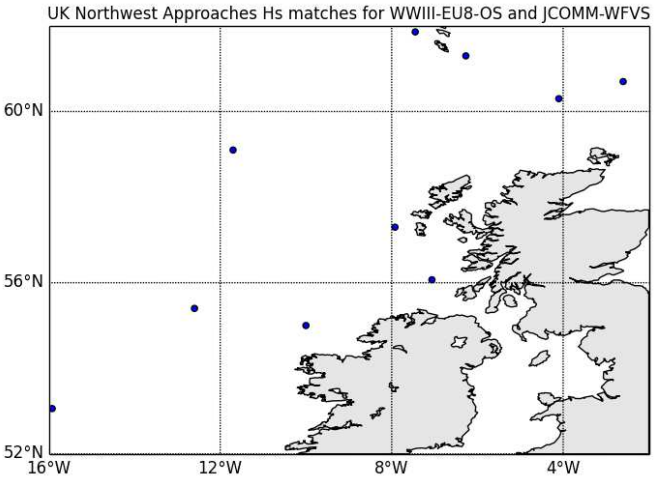

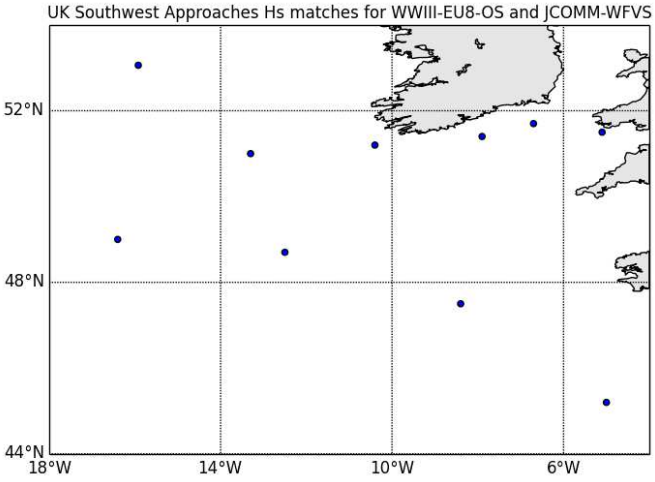

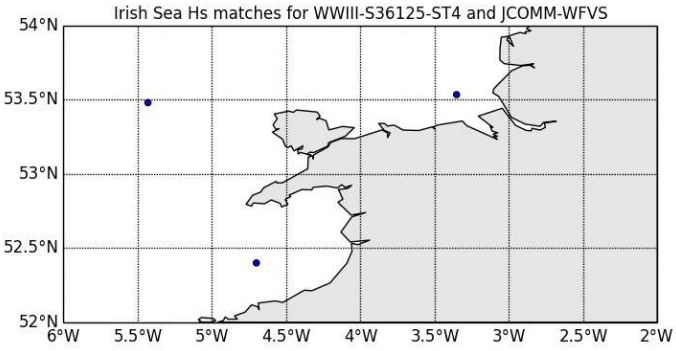

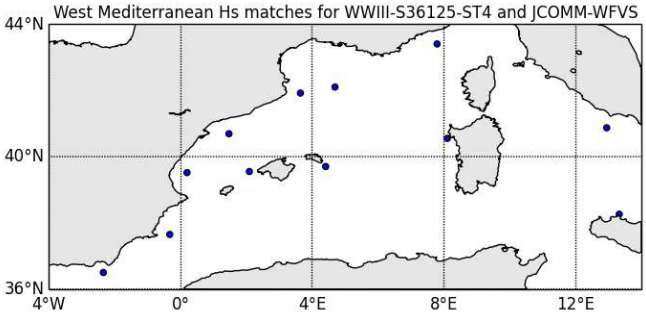

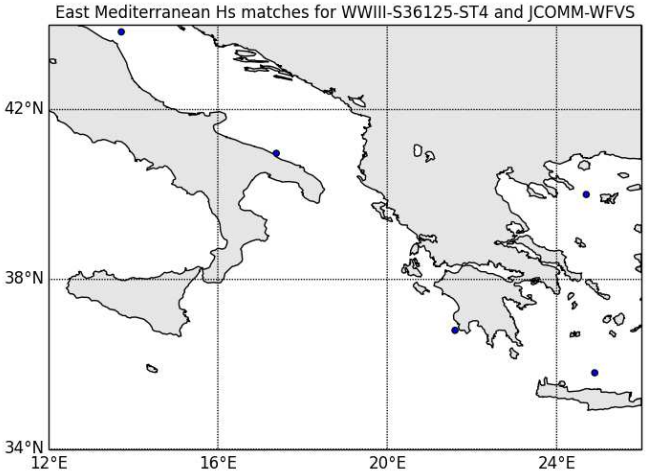

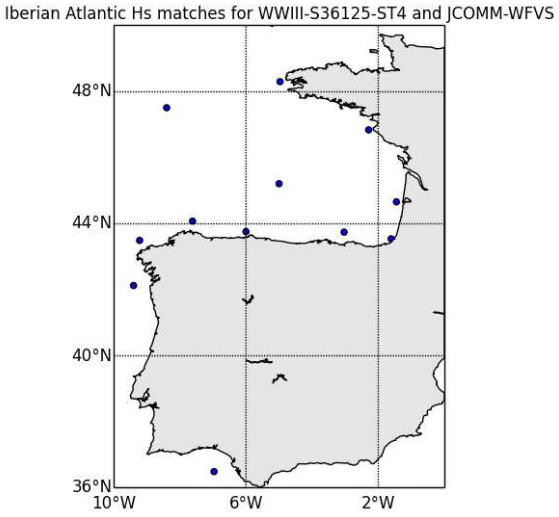

Met Office
FitzRoy Road, Exeter
Devon EX1 3PB
United Kingdom

Tel (UK): 0870 900 0100 (Int) : +44 1392 885680
Fax (UK): 0870 900 5050 (Int) :+44 1392 885681
enquiries@metoffice.gov.uk
www.metoffice.gov.uk